A Differentiated Design of Fire Exposed Steel Structures

Pettersson, Ove; Magnusson, Sven Erik; Thor, Jörgen

1974

LUND INSTITUTE OF TECHNOLOGY · LUND · SWEDEN · 1974
DIVISION OF STRUCTURAL MECHANICS AND CONCRETE CONSTRUCTION · BULLETIN 44

OVE PETTERSSON – SVEN ERIK MAGNUSSON –
JÖRGEN THOR

A DIFFERENTIATED DESIGN OF FIRE EXPOSED STEEL STRUCTURES

LUND INSTITUTE OF TECHNOLOGY · LUND · SWEDEN · 1974
DIVISION OF STRUCTURAL MECHANICS AND CONCRETE CONSTRUCTION · BULLETIN 44

SVEN ERIK MAGNUSSON - OVE PETTERSSON - JÖRGEN THOR

A DIFFERENTIATED DESIGN OF FIRE EXPOSED STEEL STRUCTURES

Presented at 1st International ECCS-Symposium "Fire Safety in Building with Steel" held on 18th and 19th October 1974 in the Hague

A DIFFERENTIATED DESIGN OF FIRE EXPOSED STEEL STRUCTURES

By Sven Erik Magnusson[a], Ove Pettersson[a], and Jörgen Thor[b]

1. Introduction

At present, a clear trend can be seen of a development of the building codes and regulations in many countries towards an increased extent of functionally based requirements and performance criteria. As concerns the design of buildings with respect to fire exposure, an essential step in the direction of such a development was taken in the Swedish Standard Specifications of 1967 [1] by introducing different alternatives of structural fire engineering design, leading to a different degree of accuracy and a different amount of engineering design work. This differentiated view of fire engineering design will be underlined further in the new edition of the standard specifications, planned to come into force during 1975.

The alternative design methods are connected to different basic characteristics of the process of fire development.

One alternative is related to the internationally prevalent standard heating curve for the gastemperature of the fire compartment combined with a subsequent cooling period, specified by a linear rate of temperature decrease which depends on the time of fire duration according to [2].

A second, more differentiated alternative is characterized by a gastemperature-time curve of the complete process of fire development which varies with the fire load density q, the ventilation characteristics of the fire compartment, and the thermal properties of the structures, enclosing the fire compartment. This basis of design is exemplified in Fig. 1a which shows the gastemperature-time curves ϑ_t-t of a certain type of fire compartment, as concerns the thermal

[a] Division of Structural Mechanics and Concrete Construction, Lund Institute of Technology, Lund, Sweden

[b] Swedish Institute of Steel Construction, Stockholm, Sweden

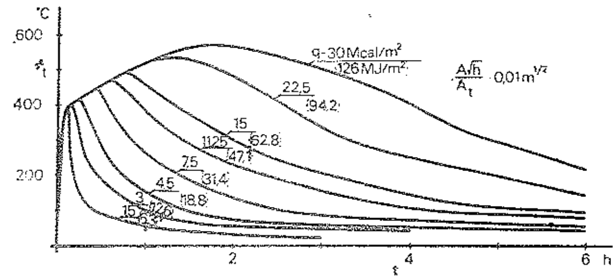

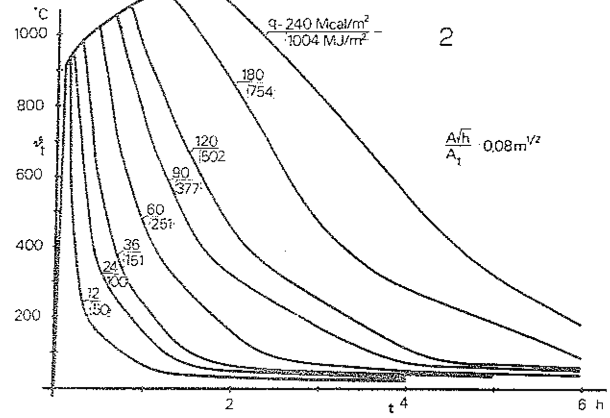

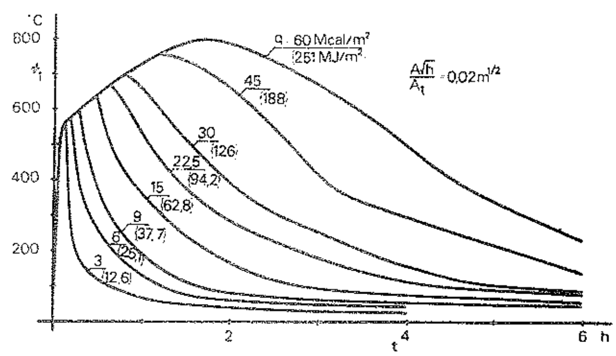

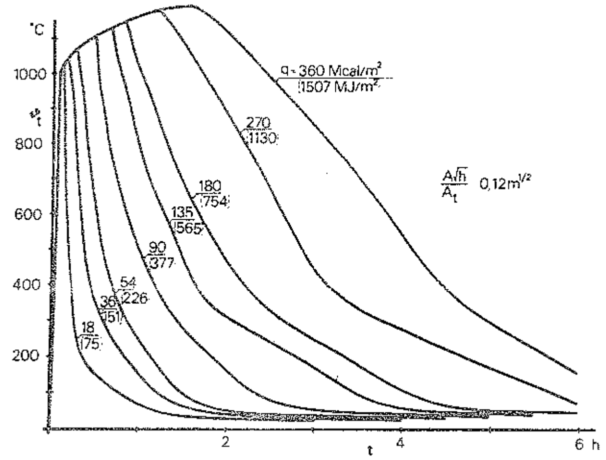

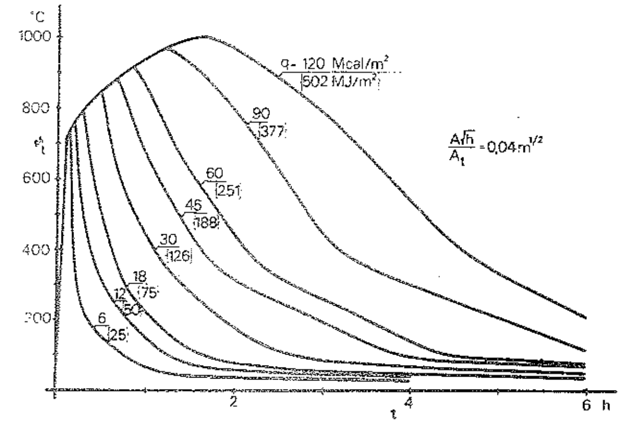

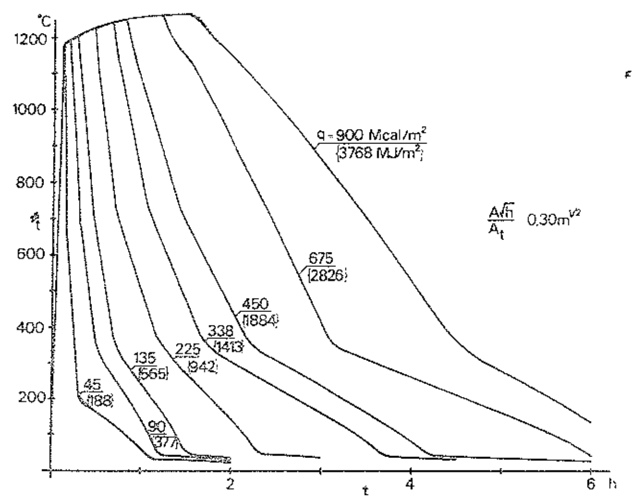

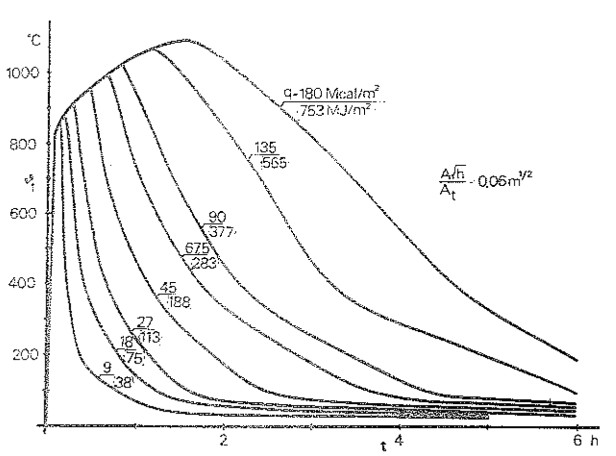

Figure 1a. Gastemperature-time curves ϑ_t-t of the complete process of fire development for different values of the fire load density q and the opening factor $A\sqrt{h}/A_t$. Fire compartment, type A, characterized by surrounding structures made of a material with a thermal conductivity $\lambda = 0.81\ W \cdot m^{-1} \cdot {}^oC^{-1}$ and a heat capacity $\rho c_p = 1.67\ MJ \cdot m^{-3} \cdot {}^oC^{-1}$

properties of the surrounding structures. The ventilation characteristics of the fire compartment are specified by the opening factor $A\sqrt{h}/A_t$, where

A_t = the total area of the interior surfaces bounding the compartment (m^2),
A = the total area of the window and door openings (m^2), and
h = the mean value of the heights of window and door openings (m) weighed with respect to each individual opening area.

This second alternative is permitted for use when the fire load is mainly of the wood fuel type.

As a third alternative, the Swedish Standard Specifications permit a structural fire engineering design on the basis of a gastemperature-time curve, calculated for each individual case from the heat and mass balance equations (Fig. 1b) - or determined in some other way - with regard taken to the combustion characteristics of the fire load, the ventilation characteristics of the fire compartment, and the thermal properties of the surrounding structures of the fire compartment.

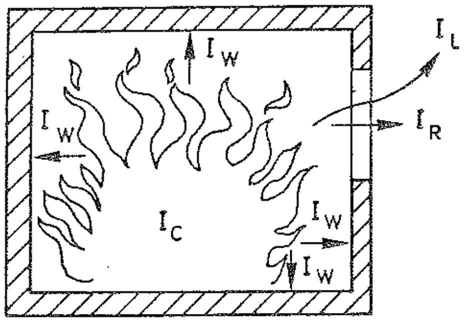

Figure 1b. Energy balance equation $I_C = I_L + I_W + I_R$ of a fire compartment. I_C is the heat release per unit time from the combustion of the fuel, and I_L, I_W, and I_R the quantities of energy removed per unit time by change of hot gases against cold air, by heat transfer to the surrounding structures, and by radiation through the openings of the compartment, respectively

In the subsequent sections, the main steps of a differentiated design of fire exposed steel structures are presented and discussed in a summary way, related to the second and third design alternative according to the Swedish Standard Specifications. Parallelly, examples are given of diagrams and tables from a comprehensive design basis, now available in Sweden [3], [4] and intended to facilitate a practical application of a differentiated fire engineering design of different types of steel structures.

2. Principles of a Differentiated Fire Engineering Design

For load-bearing structures or structural members, a differentiated design can be characterized according to Fig. 2a [5] - [8].

The basis is constituted by the characteristics of a fully developed compartment fire. Decisive entrance quantities then are

the combustion properties of the fire load,
the size and geometry of the fire compartment,
the ventilation characteristics of the fire compartment, and
the thermal properties of the structures enclosing the fire compartment.

Jointly, these quantities are determining the rate of burning, the rate of heat release, and the gastemperature-time curve of the fire compartment during the complete process of fire development.

Together with

the structural data of the proposed structure,
the thermal properties of the structural materials, and
the coefficients of heat transfer for the various surfaces of the structure

the gastemperature-time curve of the fire compartment gives the requisite information for a determination of the temperature-time fields of the fire exposed structure or structural members.

With

the mechanical properties of the structural materials, and
the load characteristics

as further entrance quantities, then a determination can be carried through of restraint forces and moments, thermal stresses, and the

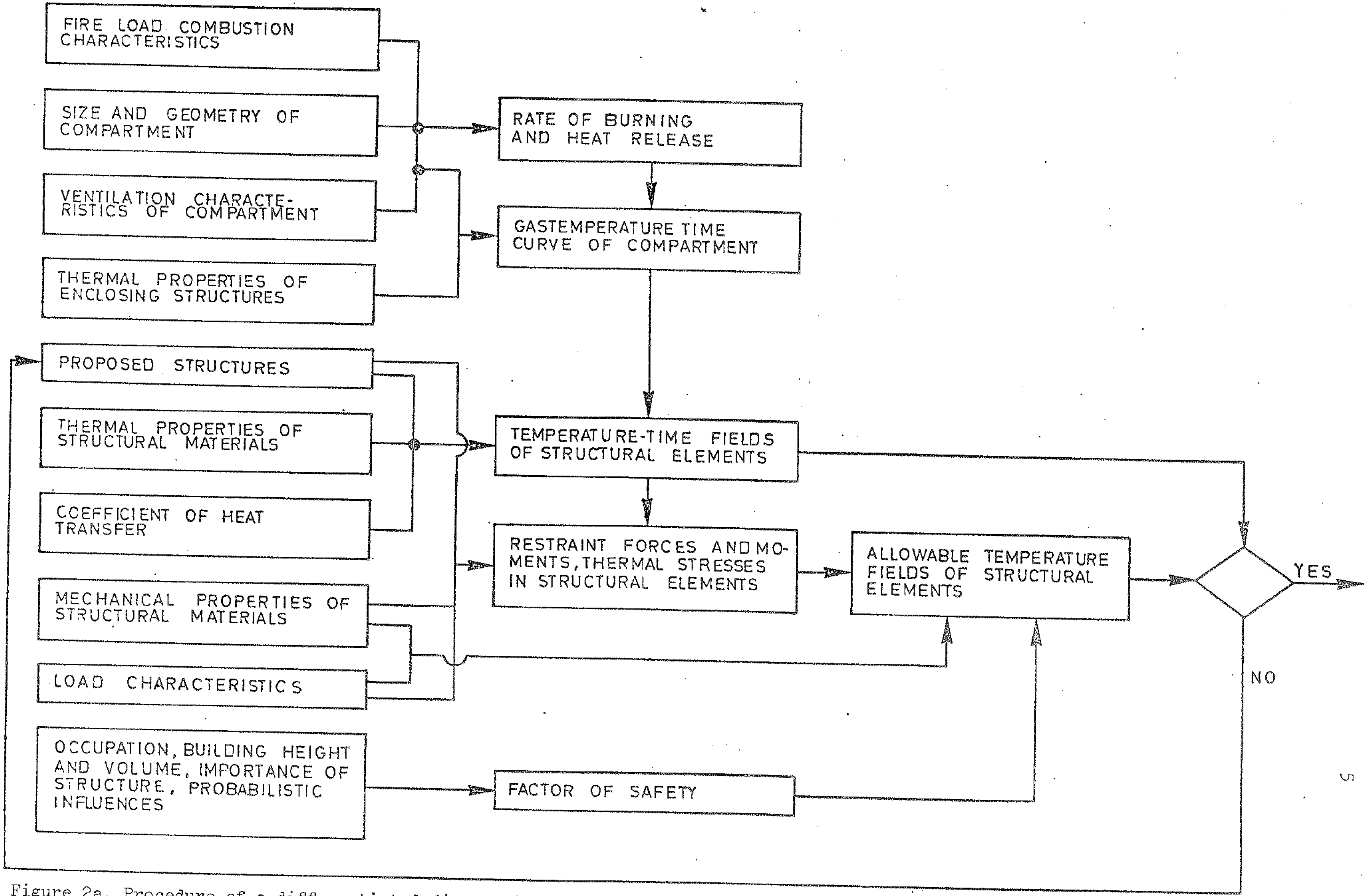

Figure 2a. Procedure of a differentiated fire engineering design of load-bearing structures or structural members

temperature fields which can be allowed with respect to the required function to be fulfilled by the structure or structural members. This determination then must be done with regard taken to a reasonably chosen level of the risk of failure introducing a factor of safety which depends on

the occupation, building height and volume, importance of structure, probabilistic influences etc.

A direct comparison between the actual temperature fields and the allowable ones decides whether the structure or the structural members investigated can fulfil their function or not at a fire exposure.

3. Structural Fire Safety

In a fire engineering design of a load-bearing structure, it is to be proved that the load-bearing capacity does not decrease below a prescribed load, multiplied by a required factor of safety, during neither the heating period nor the subsequent cooling period of the process of fire development. Summarily, the connected problem of structural safety then can be principally described in the following way.

The load-bearing structure is acted upon by a loading which, for instance, can be a combination of the dead load and a live load. This loading is characterized by a probabilistic variation which can be described by a frequency curve, comprising all those load levels L which will occur for the actual building or the actual structural member during its lifetime (Fig. 3a). At ordinary room temperature, the load-bearing structure or structural member has a load-bearing capacity B with a probabilistic variation, determined by the distribution properties of the actual structural materials and the accuracy of the actual production and described by a frequency curve. A fire exposure will give rise to a decrease of the load-bearing capacity. At a given fire compartment this decrease depends on the fire load density q, which for a given type of building or locality has a probabilistic variation with a corresponding frequency curve. Jointly, the frequency curves of the load-bearing capacity at ordinary room temperature and the fire load density constitute the basis for a determination of the frequency curve of the least load-bearing capacity at a fire exposure. In such a determination, that change in the variation of relevant structural material properties must be included, which will be caused by the heating due to the fire exposure. Further, that uncertainty must be taken into account, which at a given practical application characterizes a theoretical determination of the process of fire development, and the connected temperature-time fields and load-bearing capacity of the fire exposed structure or structural member.

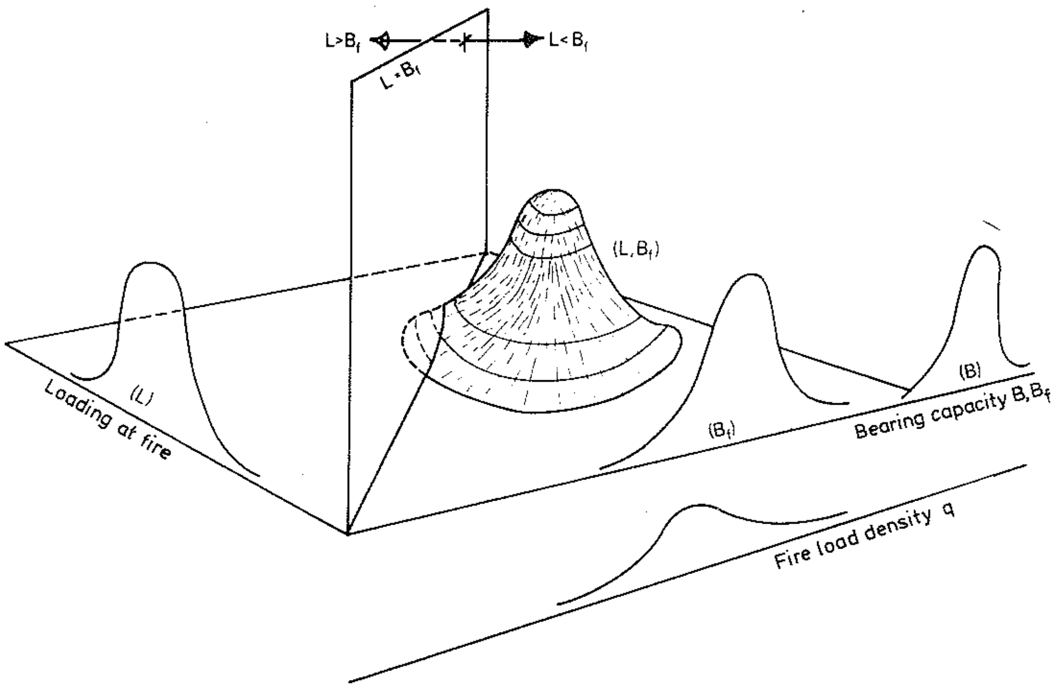

Figure 3a. Summary survey of the structural safety problem at a differentiated fire engineering design of load-bearing structures

If the frequency curve of the loading L and the frequency curve of the reduced load-bearing capacity of the fire exposed structure B_f are independent, the corresponding probability of failure at chosen levels of L and B_f can be calculated via a frequency function (L, B_f), given by a direct multiplication of the two frequency curves of L and B_f. In a presentation according to Fig. 3a, this frequency function (L, B_f) describes a surface above the horizontal L-B_f base plane. By a vertical plane L = B_f through the origin, the volume between this surface and L-B_f base plane is divided into two parts. The volume within the range L>B_f then gives the corresponding probability of failure, valid for a fire development not disturbed by any fire-fighting activities.

This probability of failure is connected to a probability = 1 for a fire outbreak leading to flashover within the actual fire compartment. As a consequence, the calculated probability of failure must be corrected by a multiplication by the probability of a fire giving flashover in the compartment for the actual structure or structural member. For this latter probability, [9] gives the following representative values:

0.3 for industrial buildings,
0.04 for office buildings, and
0.02 for residential buildings

at a lifetime of the building of 50 years. The referred values are valid for a complete building and not for a single compartment of the building. Further essential reductions of the probability of failure in fire will be caused by, for instance, an installation of detection, alarm and automatic extinguishing systems with a probabilistic variation of operation security.

A computerized procedure for an analysis of the failure probability in fire of a load-bearing structure according to the principles described above, is presented in [10]. The procedure, which is based on the Monte-Carlo method, is connected to a differentiated structural fire engineering design according to the principles outlined above. At present, the procedure can be applied in practice only in special cases. A more general application in a structural fire engineering design is for the time being rendered impossible as a consequence of insufficient knowledge concerning several of the variables entering into the procedure. In spite of these circumstances, the procedure ought to be successfully applied already, for instance, for a determination of such information which can facilitate an elaboration of prescriptions in building codes and regulations concerning reasonable levels of loading and fire load for a structural fire engineering design of load-bearing structures or structural members.

On the basis of a summary survey of the structural firesafety problem, temporary regulations now have been worked out and authorized in Sweden concerning loading values to be applied in a fire engineering design for different types of fire compartments. The loading values are connected to a load factor system and have been differentiated with respect to whether a complete evacuation of the occupants certainly can be anticipated or not - cf Table 3a.

4. Fire Load and Process of Fire Development in a Compartment

4.1. Fire Load

In most countries, the fire load (fire load density) q_c, constituting a measure of the total quantity of combustible materials in a compartment, is defined according to the relation

$$q_c = \frac{1}{A_f} \Sigma m_\nu H_\nu \qquad (\mathrm{Mcal \cdot m^{-2}}) \qquad \{\mathrm{MJ \cdot m^{-2}}\} \qquad (4.1a)$$

where A_f = the floor area (m^2), m_ν = the total weight (kg), and H_ν = = the effective heat value ($\mathrm{Mcal \cdot kg^{-2}}$) {$\mathrm{MJ \cdot kg^{-2}}$} for each individual material ν. In some countries the fire load density q_c is given alternatively as the equivalent amount of wood per unit floor area A_f.

In the current Swedish building codes and regulations the fire load density q of a compartment is defined according to the modified formula

$$q = \frac{1}{A_t} \Sigma m_\nu H_\nu \qquad (\mathrm{Mcal \cdot m^{-2}}) \qquad \{\mathrm{MJ \cdot m^{-2}}\} \qquad (4.1b)$$

where A_t = the total area of the surfaces bounding the compartment (m^2). Such a definition is more natural with respect to an application to the heat and mass balance equations of the fire compartment and primarily of that reason, this latter definition now is generally used in Sweden.

With reference to the definitions according to Eqs. (4.1a) and (4.1b), internationally a large number of probabilistic studies have been carried through of the fire load density in dwellings, offices, administration buildings, schools, stores, and hospitals. A fragmentary exemplifying of results is referred in Table 4.1a, giving a summary of the average and standard deviation of the fire load density q from recent Swedish investigations. In the table also is shown the appurtenant design fire load, corresponding to the 80 percent level of the distribution curve and authorized in Sweden as a temporary regulation.

Ordinarily, the combustion will not be complete for all fire load components at a compartment fire. This can be taken into account by determining the fire load density q from the modified formula

$$q = \frac{1}{A_t} \Sigma \mu_\nu m_\nu H_\nu \qquad (\mathrm{Mcal \cdot m^{-2}}) \quad \{\mathrm{MJ \cdot m^{-2}}\} \tag{4.1c}$$

in which μ_ν denotes a fraction between 0 and 1, giving the real degree of combustion for each individual component ν of the fire load. The coefficient μ_ν then is a function of the type of the fuel, the geometrical properties of the fuel and the position of the fuel in the fire compartment, among other things. For some types of fire load components, the coefficient μ_ν will be dependent on the time of fire duration and on the gastemperature-time characteristics of the fire compartment.

An example of a representation of fire load statistics in conformity with the idea of Eq. (4.1c) is given in Fig. 4.1a [11]. which refers some distribution curves, representative to dwellings in the suburbs and the central parts of Stockholm. In the figure the fire load density is specified on one hand by a minimum value, which only includes the highly inflammable components, and on the other hand by a maximum value, corresponding to all combustible material in the compartment, excluding floor covering.

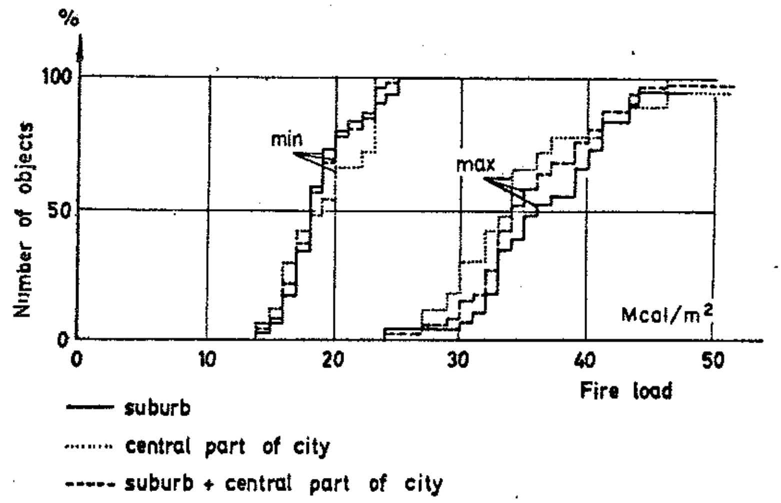

Figure 4.1a. Distribution curves for the fire load density q, defined according to Eq. (4.1b), representative to dwellings in the suburbs and the central parts of Stockholm

4.2. Characteristics of Compartment Fires

Simplified, fully developed compartment fires can be divided into two types of behaviour [12], [13] - ventilation controlled and fuel bed controlled. Ordinarily, the determination of the behaviour then is related to the average burning rate R for the active part of the fire, given as the weight loss per unit time. On the basis of results of full and model scale compartment burning tests, available from numerous reports, a plot according to Fig. 4.2a was presented in [14] of the burning rate R in the form of R/A_s versus ϕ/A_s. A_s is the initial free surface area of the fire load and ϕ a ventilation parameter, defined by the relation

$$\phi = \rho_a \sqrt{g}\, A\sqrt{h} \tag{4.2a}$$

ρ_a is the density of air and g the acceleration due to gravity. The results are based on tests with fire loads of wooden crib type.

The data, given in Fig. 4.2a, are characterized by a considerable scatter, indicating also other essential influences than those taken into account. In spite of this, two different regimes are recognizable, viz. the ventilation controlled regime, marked by an inclined line, and the fuel bed controlled regime, marked by a horizontal line. For the first type, the combustion during the flame phase is controlled by the ventilation of the compartment with the burning rate R approximately proportional to the air supply through the openings of the compartment and not in any decisive way dependent on the characteristics of the fuel. For the second type, the combustion during the flame phase is controlled mainly by the fuel bed with the burning rate R determined by the amount, porosity, and particle shape of the fuel and largely independent of the air supply through the openings.

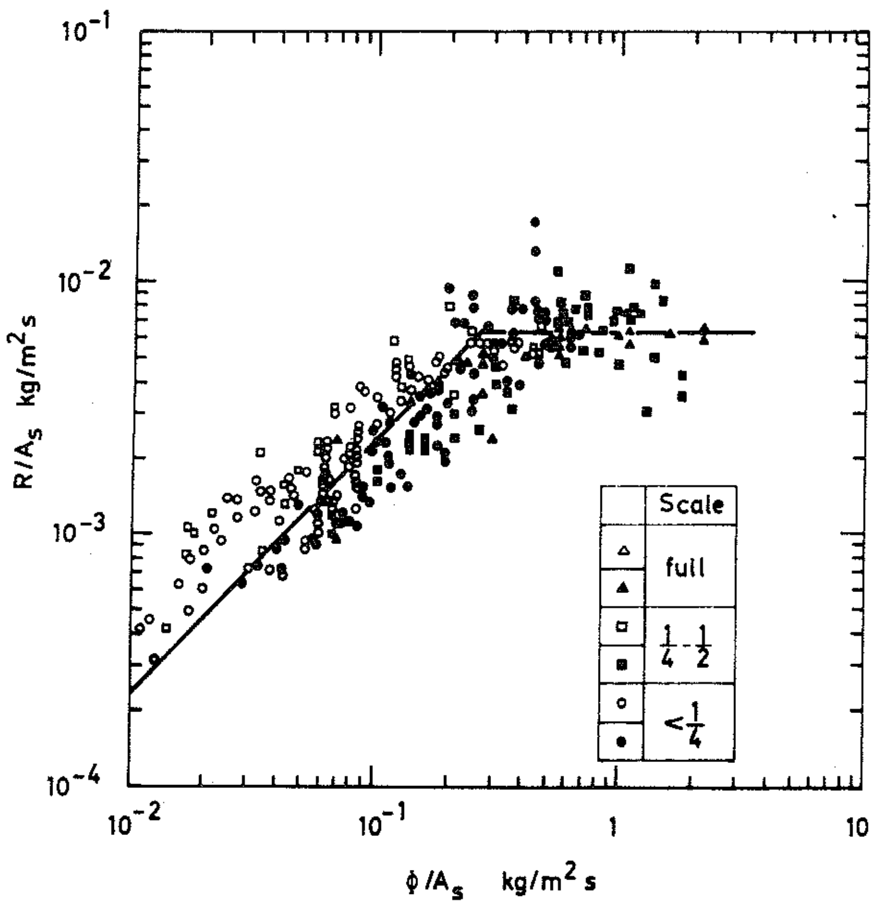

Figure 4.2a. The ratio R/A_s between the average burning rate R and the initial free surface area of the fire load A_s versus the ratio ϕ/A_s where ϕ is a ventilation parameter according to Eq. (4.2a). Fire loads of wooden crib type

For a theoretical determination of, for instance, the gastemperature-time curve of a fully developed compartment fire over heat and mass balance equations - cf [4] and [15] to [18] - a differentiated knowledge on the heat release per unit time from the combustion of the fuel I_C is of essentially higher interest than information on the burning rate R. For not well-defined fuels - for instance, fire loads of wooden type - an experimental determination of the time-variation of I_C during a complete fire process is connected to great technical difficulties and, as a consequence, for the time being direct test data are lacking on this quantity for real fire situations.

Approximately, the time curve of the rate of heat release I_C can be determined over a heat and mass balance analysis, based on the experimentally received gastemperature-time curve for compartment fires with accurately specified test conditions. Very extensive analyses of this type have been carried out in a systematic way by MAGNUSSON - THELANDERSSON [17], [18], and NILSSON [19] for fire loads of wooden crib type. As a result of these investigations, the prerequisites now exist of a differentiated theoretical determination of, for instance, the gastemperature characteristics of the complete process of a compartment fire for this type of fire load with an accuracy, which is sufficient for ordinary practical purposes. Regard then can be taken to whether a compartment fire is ventilation controlled or fuel bed controlled.

Going over from fuel of wooden crib to more realistic fire loads of furniture, it can be stated, that the results of wooden crib fires can be transferred with satisfactory accuracy for ventilation controlled fires. The main reason for this is that the burning rate and the rate of heat release are not dependent in any decisive extent on the amount, porosity and particle shape of the fuel for this type of fires. For fuel bed controlled fires, however, these fire load influences can be of great importance, which introduces considerable difficulties in transferring test data of wooden crib fires to real fire loads in practice for this type of fire. At present, the only way to consider the specific, favourable characteristics of a fuel bed controlled fire in a practical fire engineering design seems to be to calibrate at first the real furniture fire load in full scale tests, leading to, for instance, an equivalent porosity factor and an equivalent stick thickness [19]. Such systematic calibration tests for real fire loads in frequent types of fire compartments have high degree of priority.

Waiting for the results of such calibration tests, the present state of knowledge forces, as a provisional basis for a differentiated structural fire engineering design, a systematic determination of gastemperature-time curves for the complete process of compartment fires under the general assumption of ventilation control. The total energy condition of fire exposure

$$\int_0^\infty I_C \, dt = M \qquad (4.2b)$$

then always must be fulfilled, where M is the total energy content of the fire load (Mcal) {MJ}. For fuel bed controlled fires, the assumption of ventilation control together with the fulfilment of Eq. (4.2b), leads to a structural fire engineering design which will be on the safe side in practically every case, giving an overestimation of the maximum gastemperature level and a simultaneous, partly balancing underestimation of the fire duration. For the minimum load-bearing capacity or the fire resistance time of fire exposed structures or structural elements, the gastemperature- time curves determined in this way ordinarily give reasonably correct results, which has been verified in [4], [7], and [10].

An extensive basis of design, comprising differentiated gastemperature-time curves of the type mentioned for the complete process of fully developed compartment fires, is presented in [4] and [17]. Influences are the fire load density q, the opening factor of the fire compartment $A\sqrt{h}/A_t$, and the thermal characteristics of the surrounding structures. This design basis is exemplified in Fig. 1a, valid for a compartment with surrounding structures made of a material with a thermal conductivity $\lambda = 0.81\ W \cdot m^{-1} \cdot {}^oC^{-1}$ and a heat capacity $\rho c_p = 1.67\ MJ \cdot m^{-3} \cdot {}^oC^{-1}$ (fire compartment, type A). Approximately, compartments with other thermal properties of the surrounding structures can be transferred to the fire compartment, type A, via fictitious values of the fire load density q_f and the opening factor $(A\sqrt{h}/A_t)_f$ according to Table 4.2a.

The gastemperature-time characteristics, as presented in Fig. 1a and Table 4.2a, constitute a provisional, detailed basis of a differentiated fire engineering design of load-bearing structures and partitions. The chosen technique of transferring between fire compartments of different thermal properties via fictitious values of the fire load density and the opening factor has the great advantage that the computation of design diagrams and tables can be limited to the fire exposure characteristics of one type of fire compartment, viz. type A.

4.3. Opening Factor $A\sqrt{h}/A_t$

As found above, the opening factor of a fire compartment is a fundamental concept in calculating the gastemperature-time curve of the process of fire development.

For a compartment with only vertical openings, the opening factor is defined by the quantity $A\sqrt{h}/A_t$, where - cf. Fig. 4.3a

A = the total area of the window and door openings (m^2),
h = the mean value of the heights of window and door openings (m), weighed with respect to each individual opening area, and
A_t = the total interior area of the surfaces bounding the compartment, opening areas included (m^2).

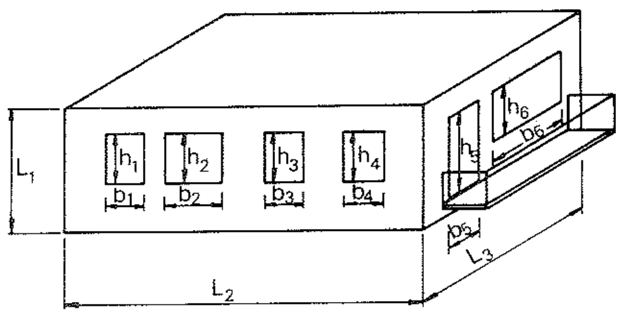

$$A = A_1 + A_2 + \dots + A_6 = b_1h_1 + b_2h_2 + \dots + b_6h_6$$
$$h = \frac{1}{A}\left[A_1h_1 + A_2h_2 + \dots + A_6h_6\right]$$
$$A_t = 2\left[L_1L_2 + L_1L_3 + L_2L_3\right]$$

OPENING FACTOR $\frac{A\sqrt{h}}{A_t}$

Figure 4.3a. Definitions of the total opening area A, the weighed mean value of the opening height h, the total interior area of the surrounding structures A_t, and the opening factor $A\sqrt{h}/A_t$ of a fire compartment

If a fire compartment also comprises horizontal openings, an equivalent opening factor $(A\sqrt{h}/A_t)_e$ can be determined by the formula [17]

$$(A\sqrt{h}/A_t)_e = f_k \, (A\sqrt{h}/A_t)_v \qquad (4.3a)$$

where $(A\sqrt{h}/A_t)_v$ is the opening factor, corresponding to the vertical openings of the compartment, calculated according to Fig. 4.3a, and f_k a dimensionless multiplier, given by the alignment chart in Fig. 4.3b. For the notations used in this chart, then see Fig. 4.3c.

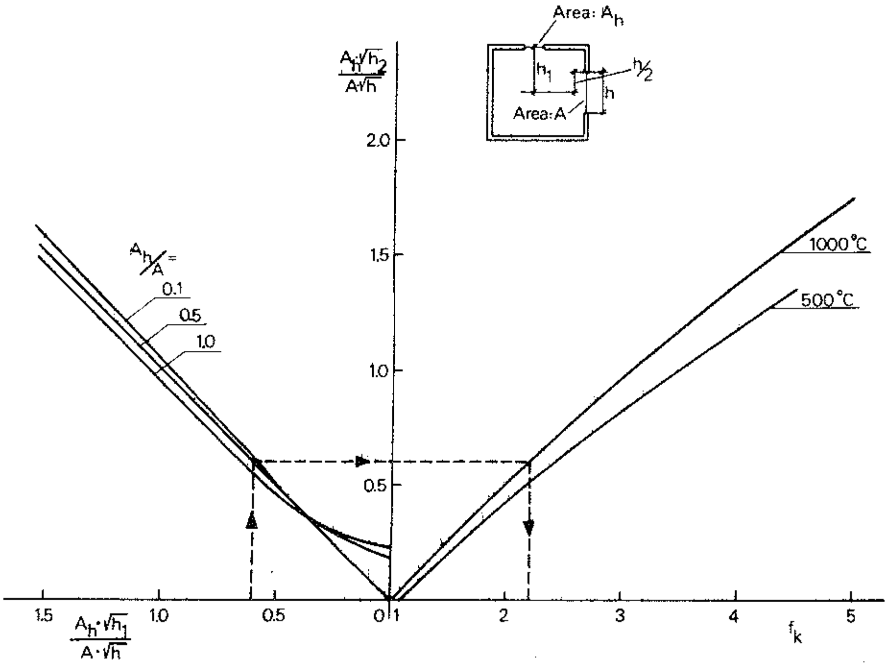

Figure 4.3b. Alignment chart for a determination of the equivalent opening factor $(A\sqrt{h}/A_t)_e$ of a fire compartment with vertical as well as horizontal openings. For notations, see Fig. 4.3c

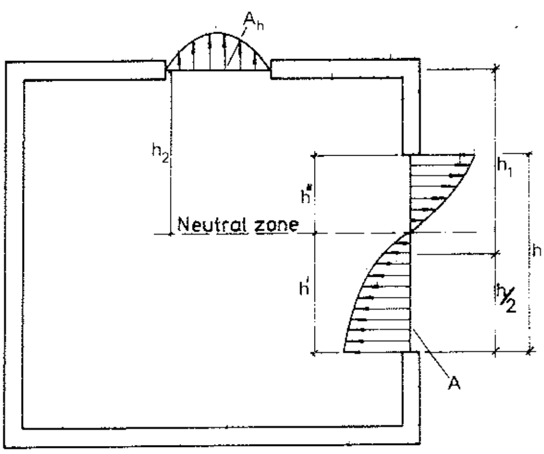

Figure 4.3c. Gas flow mechanism for a fire compartment with vertical and horizontal openings

A determination of the equivalent opening factor over Eq. (4.3a) and Fig. 4.3b presupposes that the gas flow through the horizontal openings of the roof is not predominant. This can be examined via the quotient $A_h\sqrt{h_2}/A\sqrt{h}$, which has an upper limit at which the applied gas flow model ceases to be valid. This upper limit is given by the values

$$\frac{A_h\sqrt{h_2}}{A\sqrt{h}} = \begin{cases} 1.76 \text{ at } \vartheta_t = 1000^\circ C \\ 1.37 \text{ at } \vartheta_t = 500^\circ C \end{cases} \qquad (4.3b)$$

At these limit values, the neutral zone coincides with the upper edge of the vertical opening and tests have indicated the validity of the model up to these upper limits [20].

5. Steel Temperature ϑ_s of Fire Exposed, Uninsulated Steel Structures

For a fire exposed, uninsulated steel structure, the energy balance equation directly gives the following formula for a determination of the steel temperature-time curve ϑ_s-t - Fig. 5a

$$\Delta\vartheta_s = \frac{\alpha}{\rho_s c_{ps}} \cdot \frac{F_s}{V_s} (\vartheta_t - \vartheta_s)\Delta t \qquad (^\circ C) \qquad (5a)$$

where

$\Delta\vartheta_s$ = the change of the steel temperature ϑ_s during the time step Δt,
α = the coefficient of heat transfer at the fire exposed surface of the structure,
ρ_s = the density of the steel material,
c_{ps} = the specific heat of the steel material,
F_s = the fire exposed surface of the steel structure per unit length,
V_s = the volume of the steel structure per unit length, and
ϑ_t = the gastemperature within the fire compartment.

Eq. (5a) presupposes that the steel temperature ϑ_s is uniformly distributed over the cross section of the structure at any time t and that the heat transfer is one-dimensional.

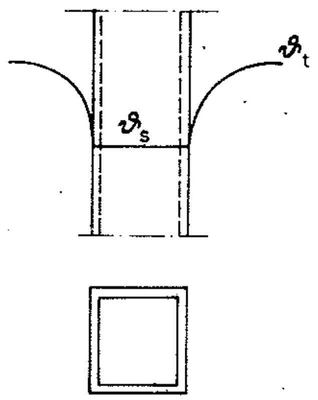

Figure 5a. Fire exposed, uninsulated steel structure. ϑ_t = gastemperature within the fire compartment, ϑ_s = steel temperature

The coefficient of heat transfer α can be calculated from the approximate formula

$$\alpha = 23 + \frac{5.77\ \varepsilon_r}{\vartheta_t - \vartheta_s}\left[\left(\frac{\vartheta_t + 273}{100}\right)^4 - \left(\frac{\vartheta_s + 273}{100}\right)^4\right] \quad (\mathrm{W\cdot m^{-2}\cdot {}^{o}C^{-1}}) \qquad (5b)$$

giving an accuracy which is sufficient for ordinary practical purposes. ε_r then is the resultant emissivity, in the case of radiation between two parallel, infinite surfaces given by the equation

$$\varepsilon_r = \frac{1}{1/\varepsilon_t + 1/\varepsilon_s - 1} \qquad (5c)$$

where

ε_t = the emissivity of flames, and

ε_s = the emissivity of the fire exposed steel surface.

For practical applications, the resultant emissivity ε_r can be chosen according to the following table, giving values which generally are on the safe side.

1. Column, fire exposed on all sides	ε_r = 0.7
2. Column, outside a facade	0.3
3. Floor structure, composed of steel beams with a reinforced concrete slab, supported on the lower flange of the beams	0.5
4. Steel beams with a floor slab, supported on the upper flange of the beams	
4a. Beams of I cross section with width/height ≥ ≥ 0.5	0.5
4b. Beams of I cross section with width/height < < 0.5	0.7
4c. Beams of box cross section and trusses	0.7

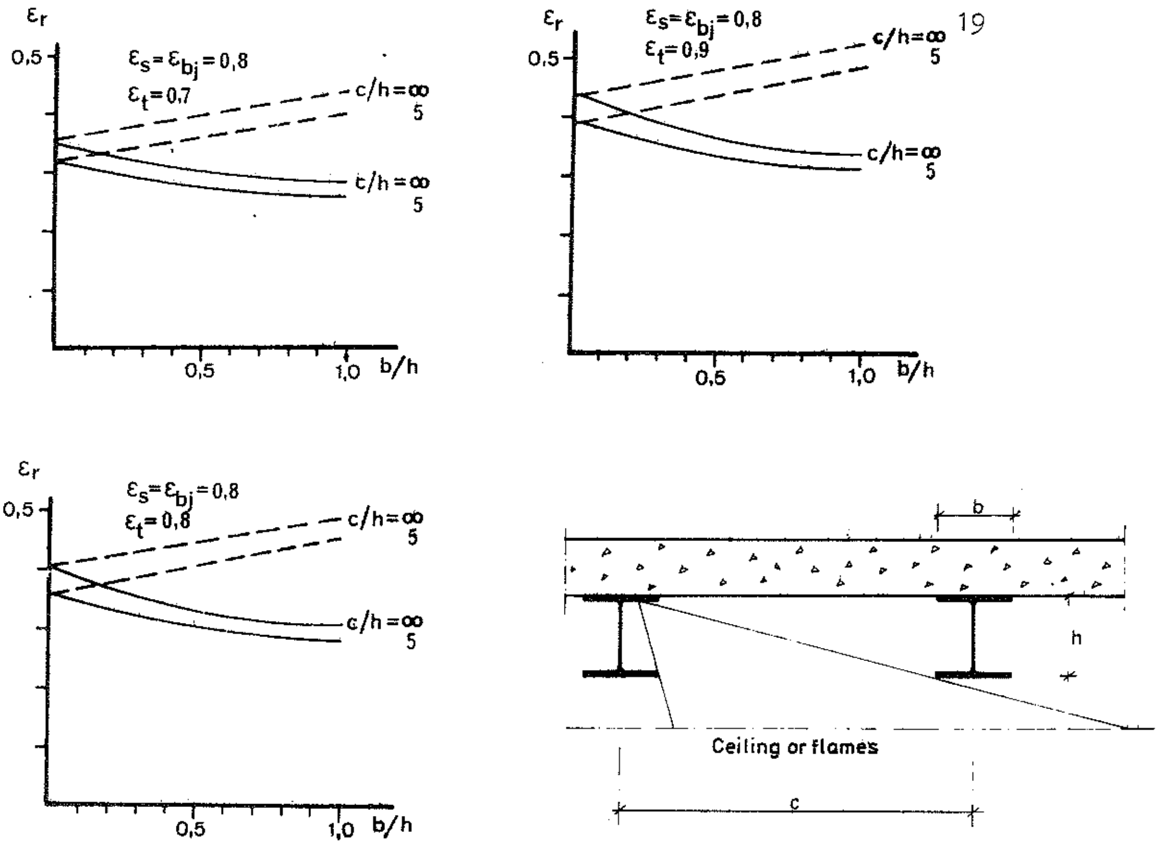

Figure 5b. Resultant emissivity ε_r for steel beams with a floor slab, supported on the upper flange of the beams. Flames completely below the steel beams.
ε_{bj} = emissivity of the slab, ε_s = emissivity of the steel beams, ε_t = emissivity of the flames.
——— I cross section, ----- box cross section

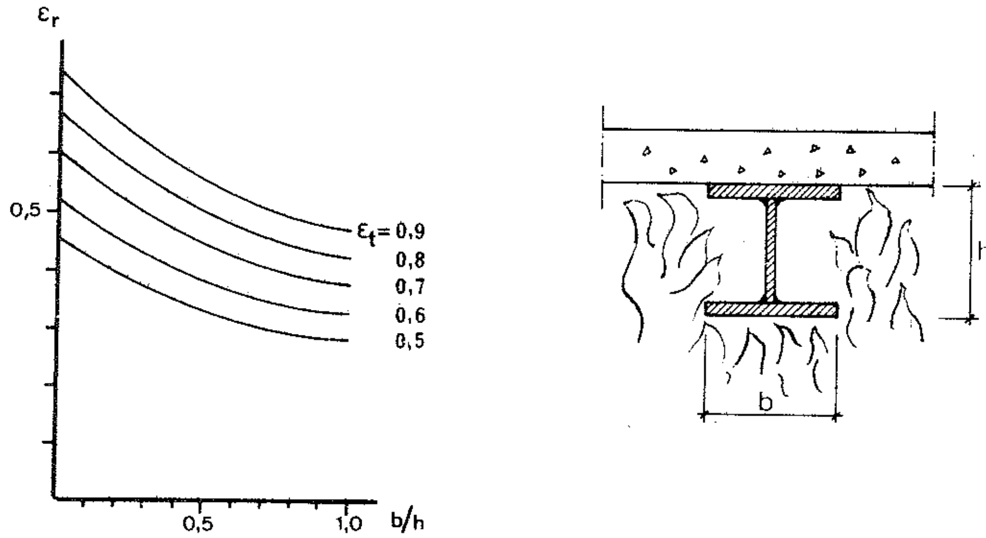

Figure 5c. Resultant emissivity ε_r for steel beams of I cross section with a floor slab, supported on the upper flange of the beams. Flames reaching the slab.
ε_t = emissivity of the flames

Column within a fire compartment

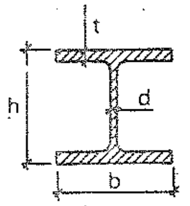

$$\frac{F_s}{V_s} = \frac{2h + 4b - 2d}{\text{cross section area}}$$

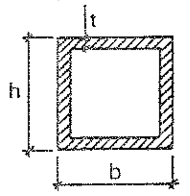

$$\frac{F_s}{V_s} = \frac{2h + 2b}{\text{cross section area}}$$

Column, immediately outside a window opening

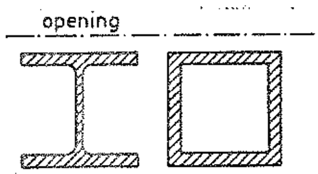

$$\frac{F_s}{V_s} = \frac{2h + b}{\text{cross section area}}$$

Floor structure, composed of steel beams with a concrete slab, supported on the lower flange of the beams

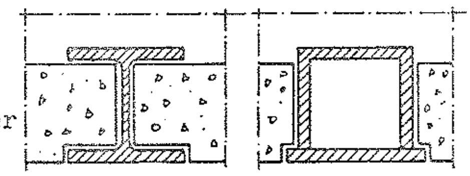

$$\frac{F_s}{V_s} = \frac{b}{bt} = \frac{1}{t}$$

Beams with a floor slab, supported on the upper flange of the beams

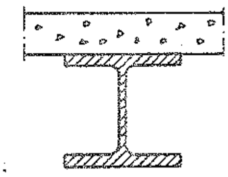

$$\frac{F_s}{V_s} = \frac{2h + 3b - 2d}{\text{cross section area}}$$

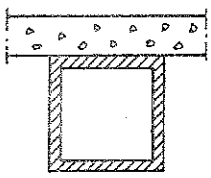

$$\frac{F_s}{V_s} = \frac{2h + b}{\text{cross section area}}$$

Floor slab beams of truss type (F_s/V_s is determined for each part of the truss)

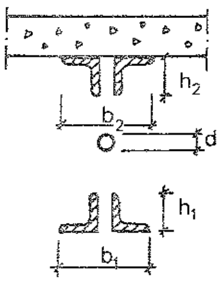

$$\frac{F_s}{V_s}\ \text{(lower flange)} = \frac{2b_1 + 2h_1}{\text{cross section area of lower flange}}$$

$$\frac{F_s}{V_s}\ \text{(upper flange)} = \frac{b_2 + 2h_2}{\text{cross section area of upper flange}}$$

$$\frac{F_s}{V_s}\ \text{(diagonal)} = \frac{4}{d}$$

Figure 5d. F_s/V_s for different types of fire exposed, uninsulated steel structures

More accurate values of the resultant emissivity ε_r can be determined for the application alternative 4 - steel beams with a floor slab, supported on the upper flange of the beams - from the diagrams of Fig. 5b and c, applicable to floor structures with the flames completely below the steel beams and reaching the slab, respectively [21] . For the emissivity of the flames ε_t, the value 0.85 is to be inserted, if not any other value can be proved to be more correct.

At a given gastemperature-time curve of the fire compartment ϑ_t-t, the steel temperature ϑ_s can be directly calculated from Eqs. (5a) to (5c) with regard taken to the temperature dependence of the specific heat of the steel and of the coefficient of heat transfer. A systematization of such computations then can result in a design basis of the type, shown in Table 5a and giving the maximum value of the steel temperature ϑ_{max} during a complete process of fire development for varying values of the fire load density q, the opening factor $A\sqrt{h}/A_t$, the structural parameter F_s/V_s, and the resultant emissivity ε_r. The values of the table are connected to gastemperature characteristics according to Fig. 1a, fire compartment type A.

Some guide-lines for the determination of the structural parameter F_s/V_s are summarized in Fig. 5d for different types of application.

6. Steel Temperature ϑ_s of Fire Exposed Insulated Steel Structures

For a fire exposed, insulated steel structure, a simplified energy balance equation gives the following relation for a direct determination of the steel temperature-time curve ϑ_s-t - Fig. 6a

$$\Delta\vartheta_s = \frac{A_i}{(1/\alpha + d_i/\lambda_i)\rho_s\, c_{ps}\, V_s}\,(\vartheta_t - \vartheta_s)\Delta t \qquad (^{\circ}C) \qquad (6a)$$

where

$\Delta\vartheta_s$ = the change of the steel temperature ϑ_s during the time step Δt,

α = the coefficient of heat transfer at the fire exposed surface of the insulation,

d_i = the thickness of the insulation,
λ_i = the thermal conductivity of the insulating material,
ρ_s = the density of the steel material,
c_{ps} = the specific heat of the steel material,
A_i = the interior jacket surface area of the insulation per unit length,
V_s = the volume of the steel structure per unit length, and
ϑ_t = the gastemperature within the fire compartment.

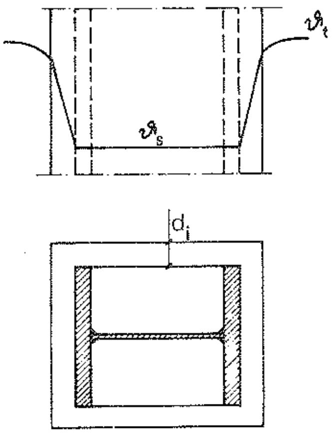

Figure 6a. Fire exposed, insulated steel structure. ϑ_t = gastemperature within the fire compartment, ϑ_s = steel temperature

Eq. (6a) presupposes that the steel temperature ϑ_s is uniformly distributed over the cross section of the structure at any time t, that the temperature gradient is linear and the heating contribution negligible for the insulation, and that the heat transfer is one-dimensional.

A somewhat more accurate formula for a numerical calculation of the steel temperature ϑ_s can be achieved by taking into account the energy corresponding to the heating of the insulation in an approximate way. By that means, the following expression can be deduced [22]

$$\Delta\vartheta_s = \frac{(\vartheta_t - \vartheta_s)\,\Delta t}{(1/\alpha + d_i/\lambda_i)\rho_s\, c_{ps}\, \frac{V_s}{A_i}\left(1 + \frac{d_i\rho_i c_{pi} A_i}{2\rho_s c_{ps} V_s}\right)} - \frac{\Delta\vartheta_t}{\frac{2\rho_s\, c_{ps}\, V_s}{d_i\, \rho_i\, c_{pi}\, A_i} + 1} \qquad (6b)$$

where not previously defined quantities are

ρ_i = the density of the insulating material, and
c_{pi} = the specific heat of the insulating material.

At a given gastemperature-time curve of the fire compartment ϑ_t-t, the steel temperature ϑ_s can be directly determined from Eqs. (5b), (5c), and (6a) or (6b). Ordinarily, then the term $1/\alpha$ can be neglected at the side of the term d_i/λ_i, indicating that variations of the resultant emissivity ε_r are of minor importance at fire exposed, insulated steel structures.

Computations, originating from Eq. (6a) or (6b), enable a construction of systematized diagrams and tables, facilitating a differentiated, structural fire engineering design in practice. An example of such a design basis is presented in Table 6a, giving the maximum value of the steel temperature ϑ_{max} according to Eq. (6a) during a complete process of fire development for varying values of the fire load density q, the opening factor $A\sqrt{h}/A_t$, the structural parameter A_i/V_s, and the insulation parameter d_i/λ_i. The values of the table are connected to gastemperature characteristics according to Fig. 1a, fire compartment type A.

The values of Table 6a were calculated on the assumption of a constant thermal conductivity of the insulating material λ_i. As a rule, however, λ_i varies with the temperature in an extent which cannot be neglected in a fire engineering design. This can be considered by applying Table 6a with a value of λ_i corresponding to an average value for the whole process of fire development. Calculations, systematically carried through, then are verifying that this average value of λ_i approximately coincides with the value, determined for an insulation temperature equal to the maximum steel temperature ϑ_{max}.

For a specific insulating material, systematized design diagrams and tables can be computed very accurately with regard taken to the temperature dependence of the thermal properties of the steel material as well as the insulating material. The influence of an initial moisture content and of a disintegration of the insulating material then can be taken into consideration, too. Practically, such a determination can be carried through over a numerical data processing by means of computers on the basis of heat balance equations, dedu-

Column in a fire compartment

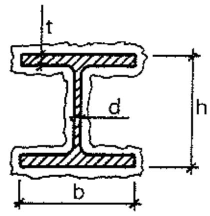

$$\frac{A_i}{V_s} = \frac{2h + 4b - 2d}{\text{steel cross section area}}$$

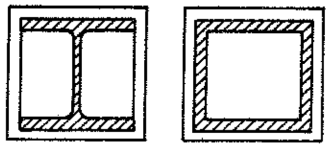

$$\frac{A_i}{V_s} = \frac{2h + 2b}{\text{steel cross section area}}$$

Column against a wall with a sufficient fire resistance

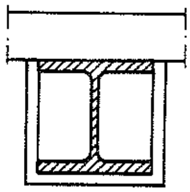

$$\frac{A_i}{V_s} = \frac{2h + b}{\text{steel cross section area}}$$

Column within a wall with a sufficient fire resistance

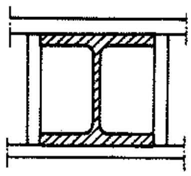

$$\frac{A_i}{V_s} = \frac{b}{bt} = \frac{1}{t}$$

Floor structure, composed of steel beams with a concrete slab, supported on the lower flange of the beams

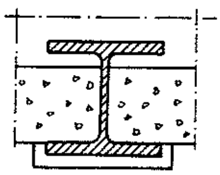

$$\frac{A_i}{V_s} = \frac{b}{bt} = \frac{1}{t}$$

Beams with a floor slab, supported on the upper flange of the beams

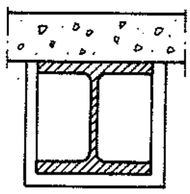

$$\frac{A_i}{V_s} = \frac{2h + b}{\text{steel cross section area}}$$

Floor slab beams of truss type (A_i/V_s is determined for each part of the truss)

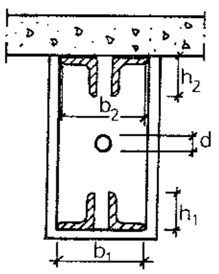

$$\frac{A_i}{V_s}\ (\text{lower flange}) = \frac{2b_1 + 2h_1}{\text{cross section area of lower flange}}$$

$$\frac{A_i}{V_s}\ (\text{upper flange}) = \frac{b_2 + 2h_2}{\text{cross section area of upper flange}}$$

$$\frac{A_i}{V_s}\ (\text{diagonal}) = \frac{4}{d}$$

Figure 6b. A_i/V_s for different types of fire exposed, insulated steel structures ced for the structure divided into finite elements. A great number of design diagrams and tables, calculated according to such an accurate procedure, are presented in [3], and [4]. Table 6b constitutes an example from this, giving the maximum steel temperature ϑ_{max} during a complete process of fire development for a fire exposed steel structure, insulated with mineral wool of density $\rho_i = 150\ kg \cdot m^{-3}$, at varying fire load density q, opening factor $A\sqrt{h}/A_t$, quotient A_i/V_s, and thickness d_i of the insulation. The gastemperature-time curves according to Fig. 1a, fire compartment type A, are the basic characteristics of the fire exposure.

The determination of the structural parameter A_i/V_s is exemplified in Fig. 6b for some different types of fire exposed, insulated steel structures.

7. Steel Temperature ϑ_s of a Fire Exposed Steel Beam Construction, Insulated with a Ceiling

A determination of the steel temperature-time curve ϑ_s-t for a steel beam construction according to Fig. 7a - composed of a reinforced concrete slab, load-bearing steel beams, and an insulating ceiling - is essentially more complicated than the corresponding determination for steel structures with an enclosing insulation. In the latter case, the gastemperature of the fire compartment ϑ_t is entering directly into the energy balance equation of the problem, cf. Eqs. (5a), (6a), and (6b). For a steel beam construction with an insulating ceiling, the surface temperature of the upper side of the ceiling and of the underneath side of the slab must be determined in a first step for enabling a calculation of the steel temperature ϑ_s in a second step.

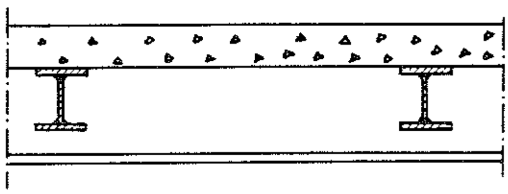

Figure 7a. Floor structure, composed of a reinforced concrete slab, load-bearing steel beams, and an insulating ceiling

A model for a determination of the temperature-time fields of a structure according to Fig. 7a, exposed to a fire from below, has been developed in [4]. The model is characterized by a division of the slab into a number of finite elements and a formulation of the energy balance equations of these elements and of the ceiling for a calculation of the time curves of the surface temperatures ϑ_{y2} and ϑ_{y3} - cf. Fig. 7b. In this first step of calculation, the heat capacity of the steel beams, the air space, and the ceiling is neglected. In the second step, the energy balance equations are formulated for the steel beams with regard to convection and to radiation from the upper side of the ceiling and the underneath side of the slab. The resultant emissivity ε_r, required for this formulation, then can be determined from Fig. 5b. The computational procedure is giving the steel temperature-time curve ϑ_s-t as the final result.

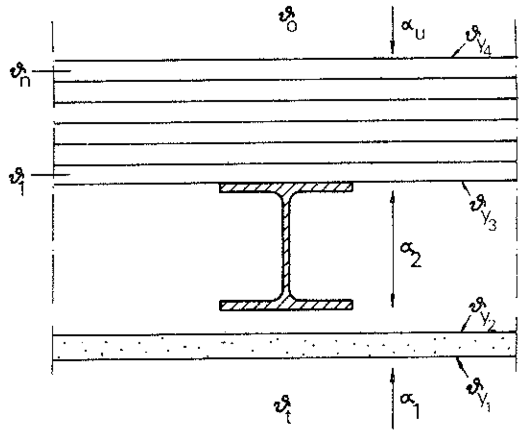

Figure 7b. Model for a determination of the temperature-time fields of a steel beam structure according to Fig. 7a, fire exposed from below

By applying this computational model in a systematic way, a design basis can be determined, facilitating a calculation of the steel temperature ϑ_s. Such a design basis is exemplified in Table 7a, giving directly the maximum steel temperature ϑ_{max} during a complete process of fire development for varying values of the fire load density q, the opening factor $A\sqrt{h}/A_t$, the structural parameter F_s/V_s, and the insulation parameter d_i/λ_i. F_s/V_s is defined according to Fig. 5d. The values within parantheses in the table, denote the corresponding maximum temperature at the centre level of the ceiling.

The values of the table are connected to gastemperature-time characteristics according to Fig. 1a, fire compartment type A.

It is to be stressed, that the design values put together in Table 7a can be applied only to a steel beam construction according to Fig. 7a with the slab made of reinforced concrete. For other slab materials, the corresponding steel temperature-time curve at a fire exposure can be quite different. This is illustrated by Fig. 7c, giving a comparison between the steel temperature-time curves ϑ_s-t, computed for the two alternatives with the slab of reinforced concrete and of lightweight concrete, density 500 kg · m^{-3}, respectively. The curves refer to a fire exposure according to the standard fire resistance test.

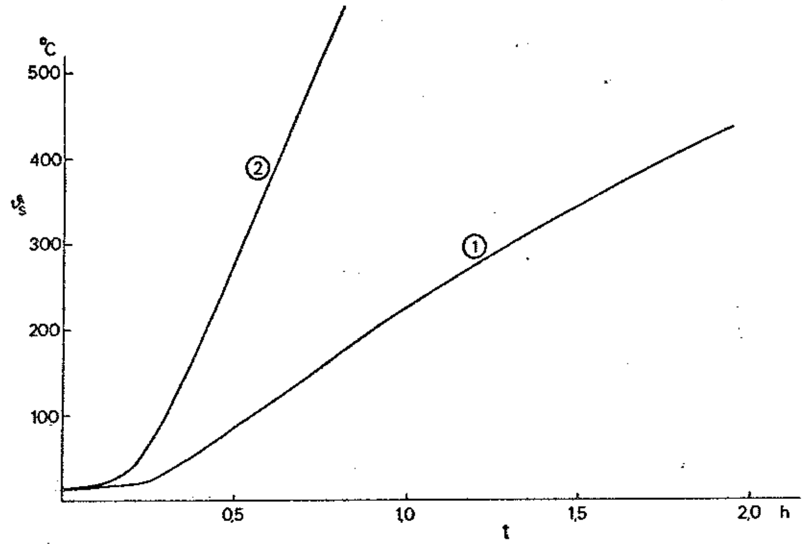

Figure 7c. Calculated time curves of the steel temperature ϑ_s-t for a steel beam construction according to Fig. 7a, fire exposed from below in conformity with the characteristics of the standard fire resistance test. Steel beams of IPE 330. Ceiling of mineral wool, density 150 kg·m^{-3}, thickness 25 mm. Slab of reinforced concrete (curve ①) or lightweight concrete of density 500 kg·m^{-3} (curve ②)

For several types of ceiling insulated steel beam constructions, the fire resistance of the ceiling and its fastening devices will be the decisive design component instead of the steel beam temperature. For instance, the ceiling can get a serious crack formation or fall down, partially or completely, after a comparatively short fire exposure. Under such conditions, the maximum steel temperature cannot be estimated solely on the basis of the thickness d_i and the thermal conductivity λ_i of the ceiling. If results are available from standard fire resistance tests, then the differentiated design problem can be solved in the following way in the cases described.

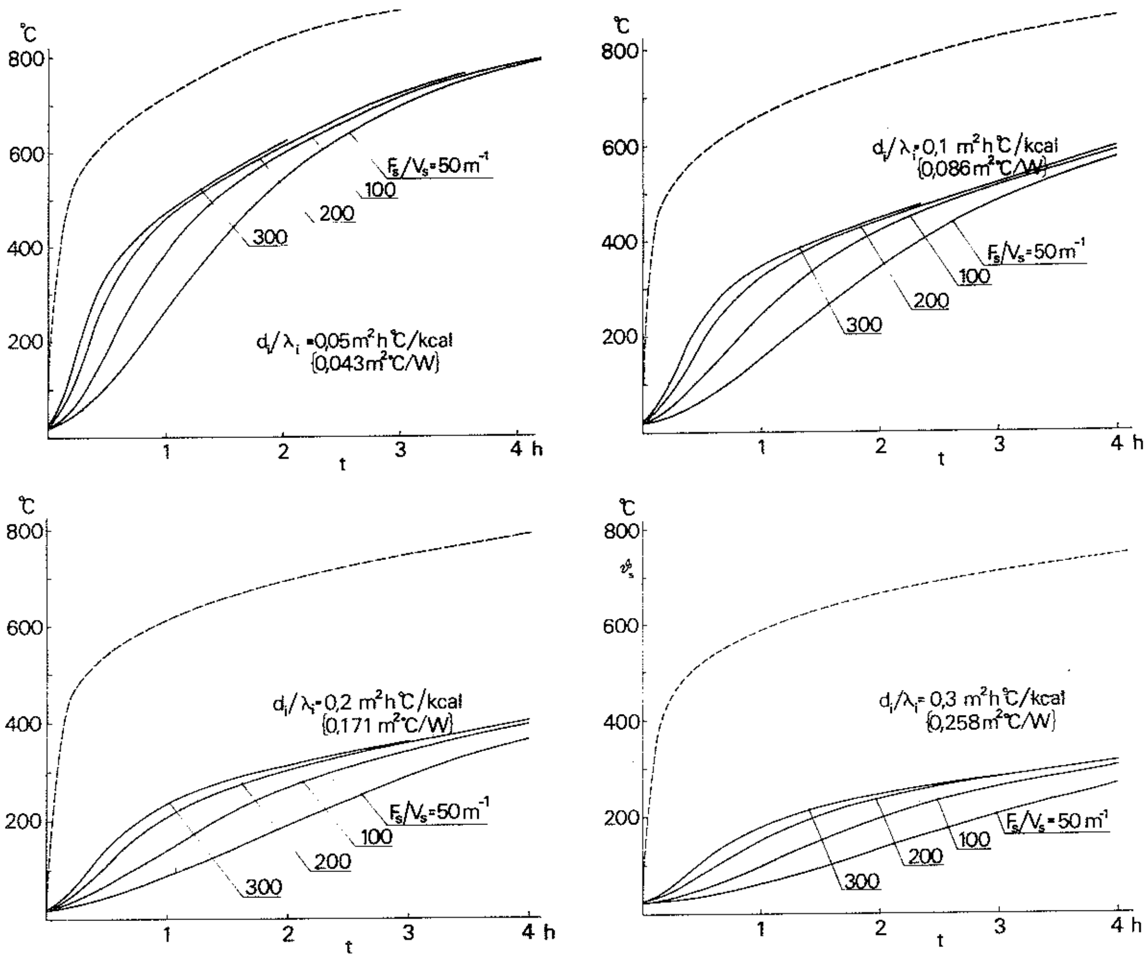

Figure 7d. Calculated time curves of the steel temperature for a steel beam construction according to Fig. 7a at varying F_s/V_s (m^{-1}) and d_i/λ_i ($m^2 \cdot h \cdot {}^oC \cdot kcal^{-1}$). Fire exposure from below according to the standard fire resistance test. The dash-line curves are giving the corresponding temperature at the centre level of the ceiling

For the actual quotient F_s/V_s, the steel beam temperature-time curve from the fire resistance test is compared with the corresponding time curves in Fig. 7d, which have been computed for really a fire exposure with a furnace temperature-time curve according to the standard fire resistance test. The comparison leads to a fictitious value of the insulation parameter d_i/λ_i – $(d_i/\lambda_i)_{fict}$ – determined from the condition that the agreement between the steel beam temperature-time curves from the test and of Fig. 7d shall be as good as possible. In the fire resistance test also can be determined the critical temperature of the ceiling with respect to its fire resistance or the intactness of its fastening devices. If such measurements have not been made, the critical temperature alternatively can be found from the dash-line curves in Fig. 7d for the actual values of F_s/V_s and $(d_i/\lambda_i)_{fict}$ by inserting the time of damage of the ceiling obtained in the test.

After the determination of the fictitious d_i/λ_i-value and the critical temperature of a ceiling, the differentiated fire engineering design can be carried out by the application of Table 7a. Parallelly, then the maximum temperature at the centre level of the ceiling according to the table is to be controlled against the critical temperature of the ceiling.

8. Load-Bearing Capacity of Fire Exposed Steel Structures

8.1. Fire Exposed Steel Structure in Bending, Tension or Compression at Negligible Risk of Buckling

A determination of the load-bearing capacity of a fire exposed steel structure in bending, tension or compression at a negligible risk of an instability failure can be carried through according to the limit state theory with the yield stress replaced by the 0.2 % proof stress. However, such a determination has certain drawbacks, since the stress-strain curves of steel are very softly rounded at elevated temperatures, giving as a consequence that the stress can often be raised considerably above the 0.2 % proof stress without the strains becoming critical. Furthermore, an estimation of the load-bearing capacity on the basis of the 0.2 % proof stress makes it difficult to take into account the creep strain of the material which begins to be noticeable for ordinary structural steels at temperatures in excess of about 450°C.

Both these influences - the softly rounded shapes of the stress-strain curves, and the creep strain - can be taken into consideration, if the load-bearing capacity is estimated on the basis of the deformations. A model has therefore been deduced for an accurate calculation of the deformation process of fire exposed steel beams [23].

In applying the model, the process of fire development is divided into a number of finite time steps and the central deflection of the beam in the beginning of each time interval is determined for the actual temperature during this interval on the basis of the stress-strain curves of the material. These curves then have been obtained in tensile tests at elevated temperatures, performed at such high rates of loading that the influence of the creep strain may be considered negligible. The effect of creep at elevated temperatures is taken into account by a separate calculation, starting from the creep equation according to DORN [24], and HARMATHY [25].

Some twenty fire tests have been performed on loaded steel beams in order to verify the calculation model. The results are exemplified in Fig. 8.1a, showing a comparison between during a fire test recorded (full-line curve) and calculated (dash-line curve) central deflections y_1 of a simply supported beam, under two symmetrically applied point loads, as a function of the time t. The temperature- time curve ϑ_s-t for the top and bottom flange at the mid-section are shown by the lower and upper chain line, respectively. The satisfactory agreement, generally obtained between calculated and recorded deflection curves, confirms the usability of the model for theoretical determinations of the deflections of fire exposed, isostatic and hyperstatic, steel beams.

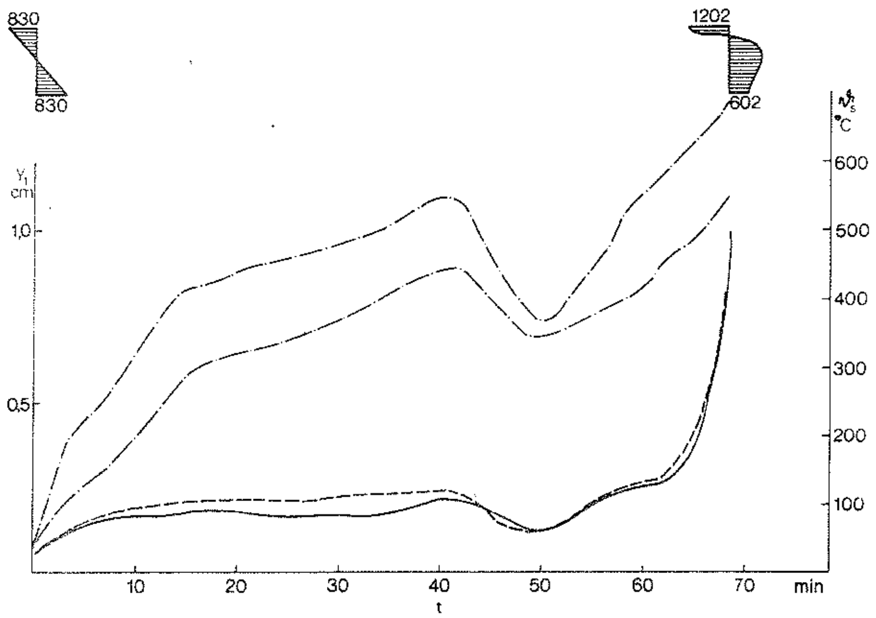

Figure 8.1a. Recorded (———) and calculated (------) time curves of the central deflection y_1 of a fire exposed, simply supported steel beam under two symmetrically applied point loads. The temperature-time curve ϑ_s-t for the top and bottom flange at the mid-section are shown by the lower and upper chain line, respectively. The insets show the calculated stress distribution at the beginning and end of the test. The curves are representative to a slow process of fire development

Principally, the load-bearing capacity of a fire exposed beam can be considered exhausted when its rate of deflection is infinitely high. However, such a failure criterion is impossible to use in a practical design based on real fire characteristics, especially if the influence of creep at elevated temperatures is to be taken into account which means that the deflection of the beam continues to increase during its cooling down period. From a practical point of view, it is necessary to use a failure criterion connected to a finite deflection or a finite rate of deflection. Experimental and theoretical investigations then have confirmed that the deflection criterion according to ROBERTSON and RYAN [26] is suitable to be applied to fire exposed steel beams. For a fire exposed beam, loaded by a constant bending moment along its entire length, this deflection failure criterion is equivalent to a strain of 0.5 % at the bottom of the beam. For a simply supported beam under a uniformly distributed load, the corresponding strain at the bottom of the midspan cross section is 0.8 to 1.0 %, and for a simply supported beam under a central point load 1.5 to 1.9 % [23]. The range of variation of the referred strain values then reflects the influence of varying maximum temperature and rate of heating.

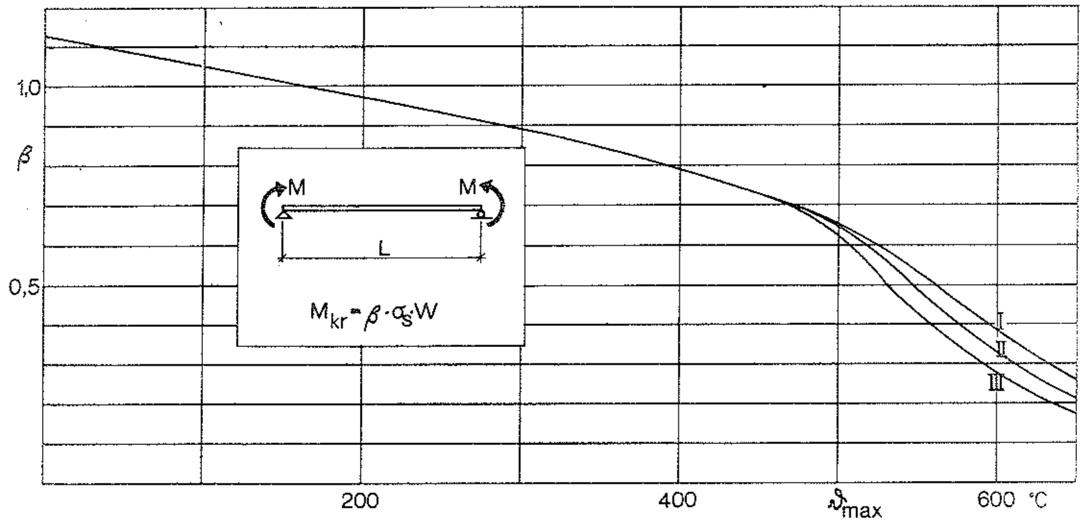

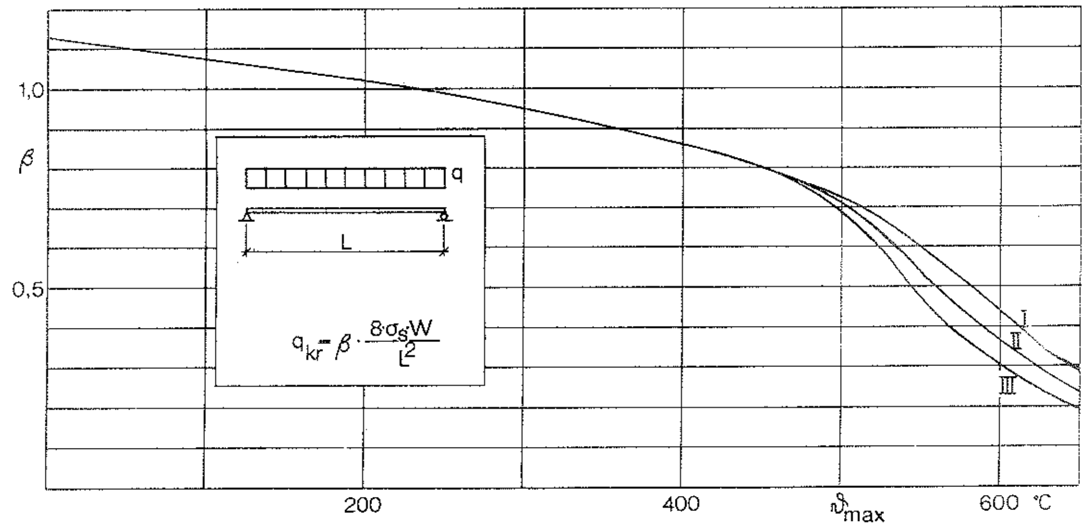

Figure 8.1b. Diagrams for a determination of the load-bearing capacity (M_{kr}, q_{kr}) for two different types of loading at a simply supported steel beam of constant I cross section. The curves I, II and III correspond to different rates of heating and subsequent cooling according to the definitions in the text. σ_s is the yield point stress at ordinary room temperature and W the elastic modulus of the cross section

By a systematized approach according to the principles, outlined above, design diagrams have been computed for a direct determination of the load-bearing capacity (critical loads) of fire exposed steel beams for different loading and support conditions at varying values of the maximum steel temperature ϑ_{max}. The diagrams are exemplified in Fig. 8.1b for two different types of loading at a simply supported beam of constant I cross section. The diagrams are differentiated with respect to the rates of heating and subsequent cooling above a steel temperature of about 450°C, which means that the influence of creep at elevated temperatures is included. The curves I, II and III correspond to a rate of heating of 100, 20 and 4°C per minute, respectively, and a rate of cooling which is 1/3 of the rate of heating.

The rate of heating can be roughly estimated with the help of Fig. 8.1c which gives the average rate of heating of the beam a as a function of the fire load density q for different values of the opening factor $A\sqrt{h}/A_t$ and the maximum steel temperature ϑ_{max}.

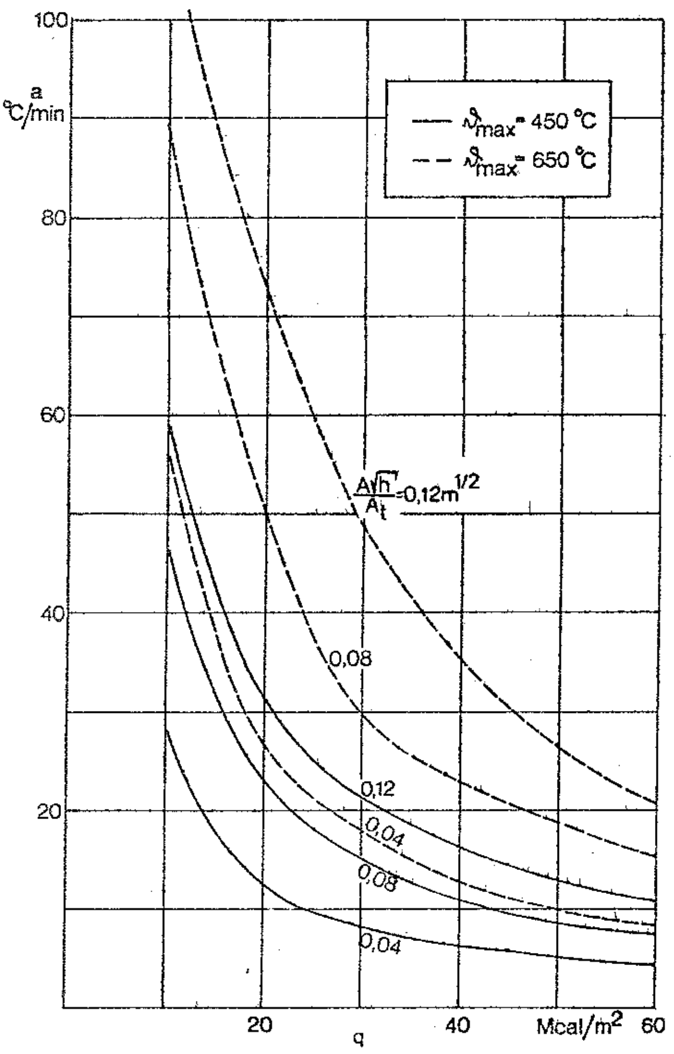

Figure 8.1c. Average rate of heating a of a fire exposed, uninsulated or insulated, steel beam as a function of the fire load density q for different values of the opening factor $A\sqrt{h}/A_t$ and the maximum steel temperature ϑ_{max}

8.2. Buckling Load of Fire Exposed Steel Columns

As concerns structural design methods with respect to buckling of axially compressed steel columns at ordinary room temperature, the present state on the whole can be characterized by two main groups of methods.

For the methods of the first main group, the following fundamental way of tackling the problem then is representative. In a first step, the buckling load $\bar{N}_k$ is determined for the idealized case of a centrically compressed, initially straight column with the real stress-strain curve of the material taken into account. In the second step, the corresponding permissible compressive load $\bar{N}_{k,perm}$ is calculated by dividing the buckling load $\bar{N}_k$ with a safety factor s. For an adaptation to real practical conditions, this safety factor must include the influences of practically representative imperfections of the column and of unintentional eccentricities of the load. This leads to a safety factor which varies with the slenderness ratio of the column.

In the methods of the second main group, the buckling load N_k is determined directly on the assumption of a column with an imperfection and a compressive load with an unintentional eccentricity which are representative for practical conditions. For this case, the maximum compressive stress σ_{max} of the column is calculated with the influence of additional deflections taken into account. As critical with regard to the load-bearing capacity, that compressive load N_k is defined for which σ_{max} reaches a decisive value, ordinarily the yield point stress σ_s or the 0.2 % proof stress $\sigma_{0.2}$. The permissible compressive load $N_{k,perm}$ then is given by dividing the buckling load N_k by a safety factor s_o which is independent of the slenderness ratio of the column.

For a theoretical determination of the buckling load or the critical temperature with respect to buckling of a fire exposed steel column, an attachment to the second group of methods comes natural. This is especially obvious for a theoretical analysis of a column with a partial restraint to longitudinal expansion during the fire.

For a fire exposed column without any restraint to longitudinal expansion, the buckling compressive stress

$$\sigma_k = \frac{N_k}{A} \tag{8.2a}$$

can be determined from the formula

$$\sigma_k^2 - \sigma_k \left[\sigma_{0.2} + \pi^2 E \left(4.8\cdot 10^{-5} + \frac{1}{\lambda^2}\right)\right] = -\sigma_{0.2}\,\frac{\pi^2 E}{\lambda^2} \qquad (8.2b)$$

The formula presupposes a material, for which the stress-strain relation can be approximated in a satisfactory way by a stress-strain diagram for a perfectly elastic-plastic material. In the relation, the total amount of the initial deflection of the column and the unintentional load eccentricity is taken into consideration by assuming only an initial deflection with the same mathematical form as the ideal buckling deflection and with a maximum value f of [27]

$$f = 4.8\cdot 10^{-5}\,\frac{(\beta L)^2}{d} \qquad (8.2c)$$

In Eqs. (8.2a) to (8.2c)

A = the cross section of the column,
E = the modulus of elasticity in the corresponding, perfectly elastic-plastic stress-strain diagram for actual steel temperature ϑ_s,
$\sigma_{0.2}$ = the 0.2 % proof stress for actual steel temperature ϑ_s,
L = the length of the column,
βL = the equivalent buckling length of the column, referred to the EULER buckling case with hinged ends of the column,
β = a dimensionless coefficient, which depends on the end conditions and the variation along the column of the cross section and of the axial load, and which directly can be taken from ordinary manuals in a large number of cases,
d = the distance from the gravity centre axis to the edge of that cross section of the column with maximum compressive stress,
λ = the equivalent slenderness ratio of the column, defined by the formula

$$\lambda = \frac{\beta L}{i} \qquad (8.2d)$$

i = the radius of gyration of the cross section with regard to bending of the column in the plane of buckling.

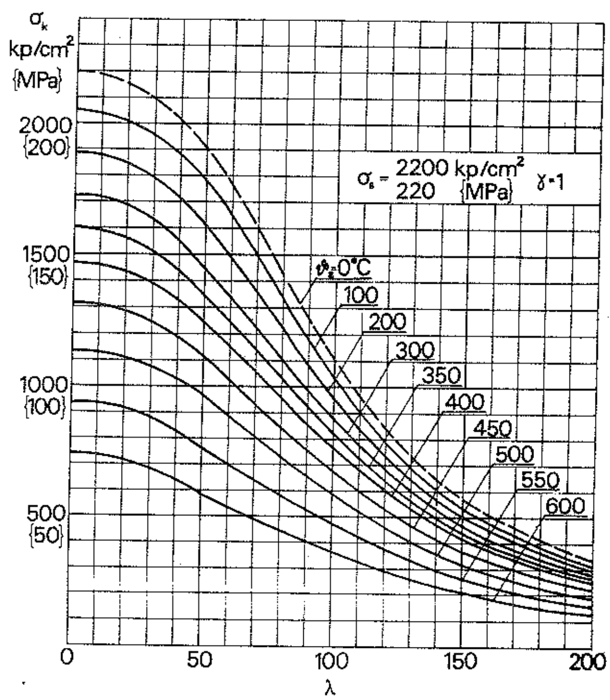

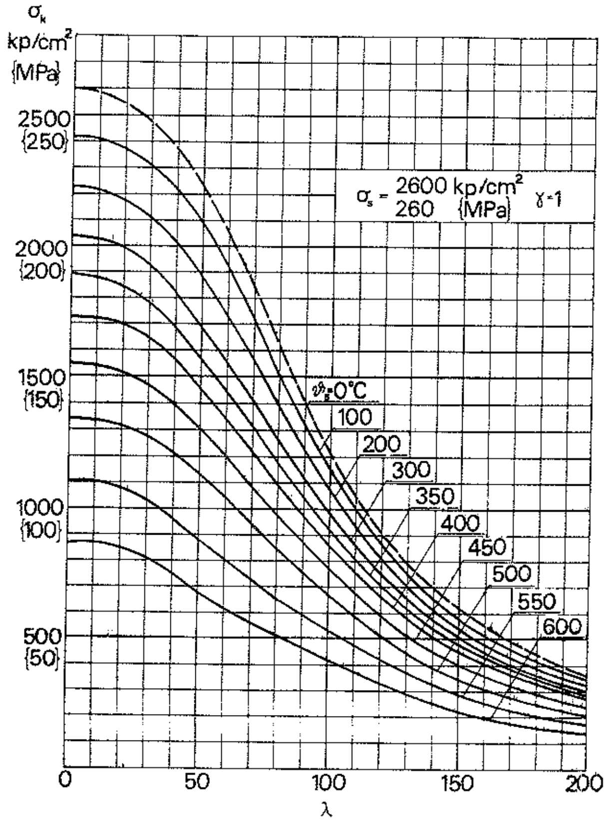

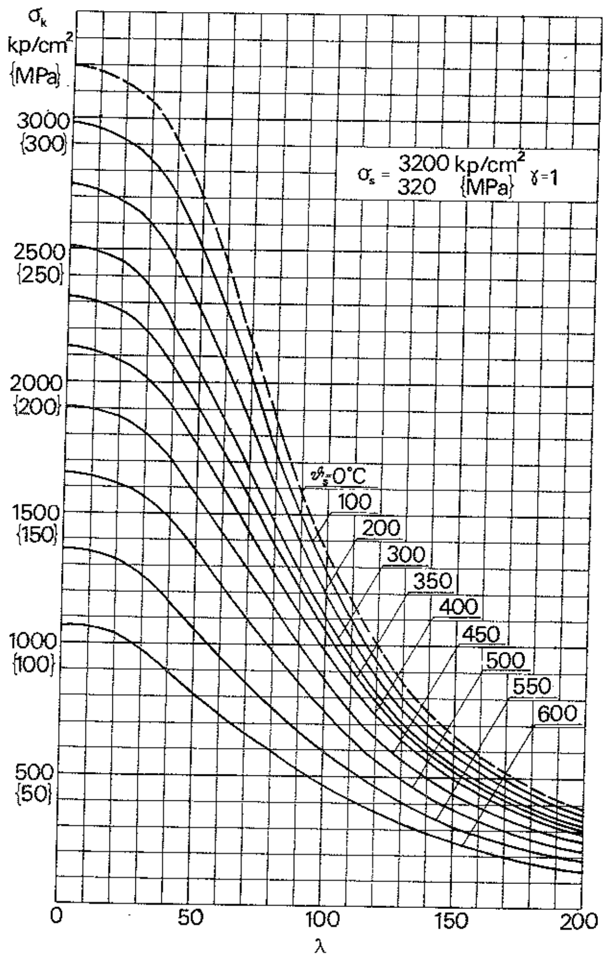

Figure 8.2a. Variation with the steel temperature ϑ_s of the relationship between the buckling stress σ_k and the equivalent slenderness ratio λ for fire exposed, axially compressed steel columns, free to expand longitudinally and made of steel with a yield point stress at ordinary room temperature σ_s = = 2 200, 2 600 and 3 200 kp/cm², respectively

After an approximation of the real stress-strain curves for different steel temperatures ϑ_s by corresponding stress-strain diagrams of a perfectly elastic-plastic material, the buckling compressive stress σ_k can be determined for a fire exposed steel column without any longitudinal restraint by solving Eq. (8.2b) [3], [22]. As a consequence of the softly rounded form of the stress-strain curves of steel at elevated temperatures, functionally better based values of the buckling compressive stress σ_k are obtained if the initial modulus of elasticity E and the 0.2 % proof stress $\sigma_{0.2}$ are replaced by the secant modulus and the 0.5 % proof stress $\sigma_{0.5}$ at the evaluation of Eq. (8.2b). Design diagrams, calculated in this way are exemplified in Fig. 8.2a for axially compressed columns made of steel having a yield point stress at ordinary room temperature σ_s = 2 200, 2 600 and 3 200 kp/cm^2, respectively. For steel qualities with intermediate σ_s-values, the design diagrams can be applied over a linear interpolation. The buckling stress σ_k is given as a function of the steel temperature ϑ_s and of the equivalent slenderness ratio of the column λ.

The diagrams are based on a temperature and stress level dependence for the secant modulus E and the 0.5 % proof stress $\sigma_{0.5}$ according to Fig. 8.2b. These material quantities then have been received in tension tests at a very slow loading rate which implies that a considerable effect of short-time creep has been included.

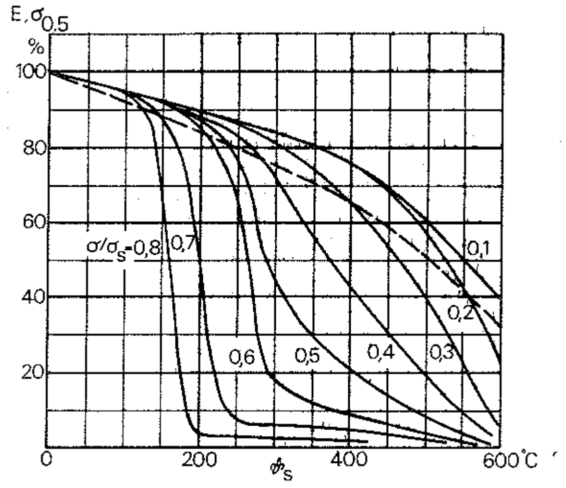

Figure 8.2b. Secant modulus E as a function of the steel temperature ϑ_s at varying stress level σ/σ_s where σ_s is the yield point stress at ordinary room temperature (full-line curves). 0.5 % proof stress $\sigma_{0.5}$ as a function of the steel temperature ϑ_s (dash-line curve)

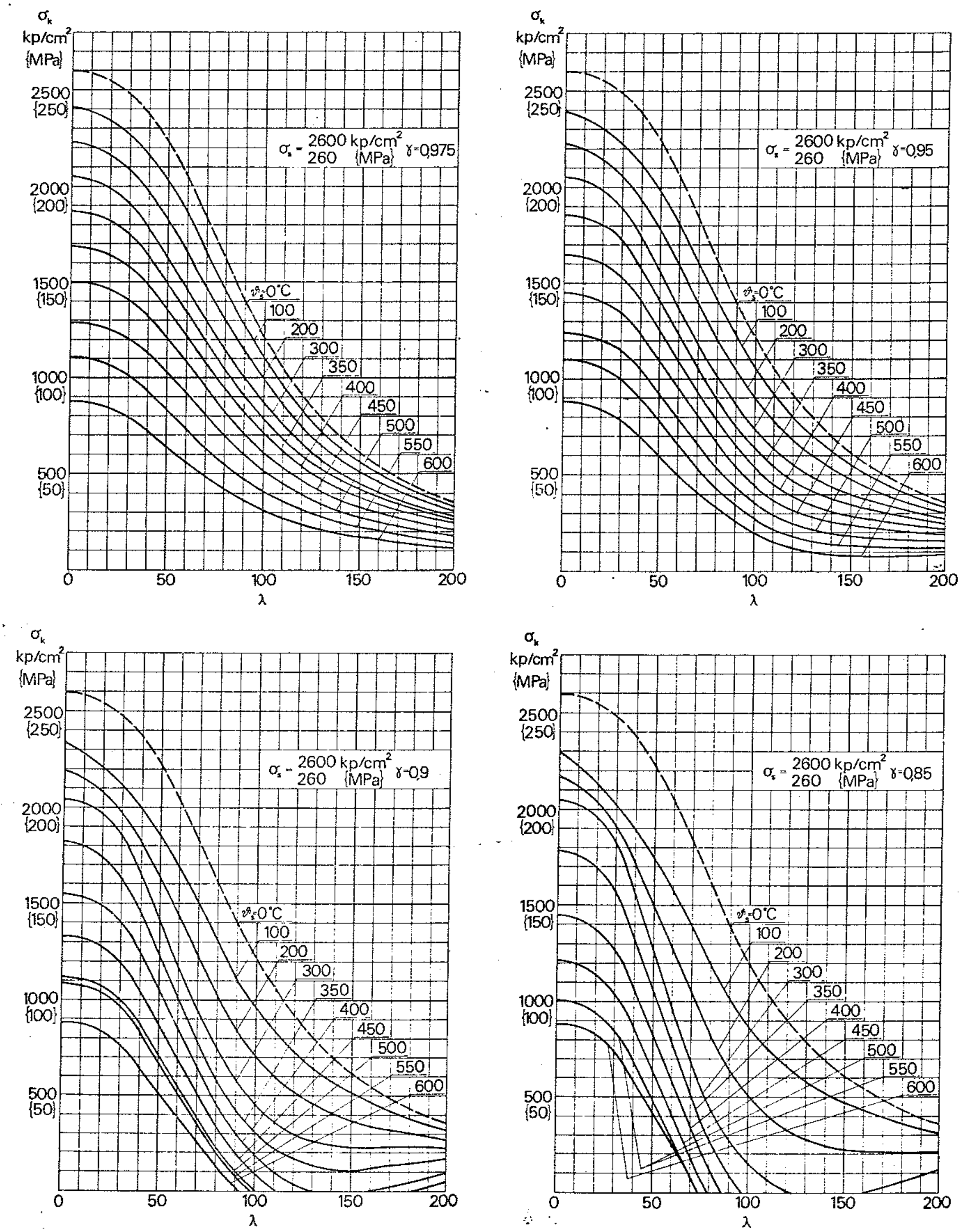

<u>Figure 8.2c</u>. Variation with the steel temperature ϑ_s of the relationship between the buckling stress σ_k and the equivalent slenderness ratio λ for fire exposed, axially compressed steel columns, partially restrained to longitudinal expansion and made of steel with a yield point stress at ordinary room temperature σ_s = $= 2\ 600\ kp/cm^2$

With the actual, equivalent slenderness ratio of the column λ and the actual design load in connection with a fire exposure, $\sigma_a = \sigma_k$, as entrance quantities, the diagrams in Fig. 8.2a directly give the critical steel temperature $\vartheta_{s_{cr}}$. As a design criterion, it is to be proved that this critical steel temperature $\vartheta_{s_{cr}}$ at least is as much as the maximum value of the actual steel temperature ϑ_{max} during the fire exposure. This maximum steel temperature ϑ_{max} then directly can be taken from the Tables 5a, 6a and 6b.

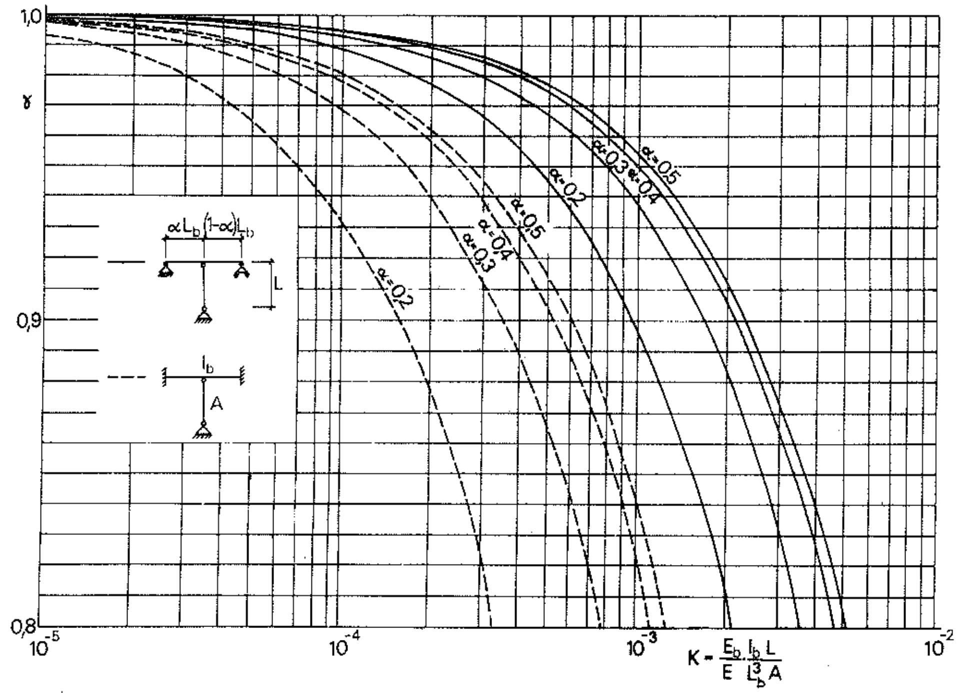

Figure 8.2d. The coefficient γ, defining the degree of axial restraint for a fire exposed column, exemplified for a simply supported or a built in beam as the adjoining structure. In the dimensionless parameter K, E_b is the modulus of elasticity of the beam for actual steel temperature ϑ_s, E the secant modulus of the column for actual steel temperature ϑ_s and actual stress level σ/σ_s (Fig. 8.2b, additional stress from the axial restraint included), L_b the total length of the beam, L the column length, I_b the moment of inertia of the beam and A the cross section of the column

The design curves in Fig. 8.2a are valid under the presumption that the column is unrestrained with respect to longitudinal expansion during the fire. A complementary illustration of the influence on the buckling stress σ_k of a partial restraint to longitudinal expansion is given in Fig. 8.2c [28], valid for a fire exposed column of steel having a yield point stress at ordinary room temperature

σ_s = 2 600 kp/cm^2. The different diagrams then refer to varying degree of axial restraint, characterized by a dimensionless coefficient γ, giving the quotient between the possible longitudinal expansion and the completely unrestrained elongation of the fire exposed column. Accordingly, γ = 1 corresponds to no longitudinal restraint at all, and γ = 0 to a full restraint to axial expansion of the column. For $\gamma \neq 1$ the σ_k-λ relationship varies with the quotient i/d, and the curves reproduced are for i/d = 0.5.

The coefficient of longitudinal restraint γ is determined by the quotient between the stiffness of the column and the stiffness of the adjoining structures in connection with the fire exposure. An example of a design diagram, facilitating a determination of the restraint coefficient γ is shown in Fig. 8.2d.

Summary

A differentiated procedure is presented for a fire engineering design of load-bearing steel structures. The procedure is a direct design method based on gastemperature-time characteristics of the process of fire development which depend on the fire load, the ventilation of the fire compartment and the thermal properties of the structures enclosing the fire compartment.

For the practical application of the design procedure, a manual has been worked out comprising a comprehensive design basis in the form of diagrams and tables which directly are giving the maximum steel temperature for a differentiated complete process of fire development and the corresponding load-bearing capacity. The design basis is fragmentarily exemplified in this paper, primarily for giving a rough impression of the character of the manual and the differentiated design procedure. The practical use of the manual has been approved by the National Board of Urban Planning in Sweden.

The differentiated design procedure presented is to be seen as an attempt to build up a logical system for a structural fire engineering design, based on functional requirements. Fundamentally, such a sys-

tem is in agreement with the present development of building codes and regulations. It is well devoted to stimulate the architects and the structural engineers to solve the fire engineering problems in a qualified way over a design procedure which is equivalent to the design procedure, conventionally applied with respect to, for instance, static loading. The presented design system is not homogeneous, as regards the present basis of knowledge for the different design steps, which could be put forward as a criticism of the system. However, such a remark is not essential. Instead, this fact ought to be used as an important information on how to systematize a future research for enabling a successive improvement of the system.

References

[1] Svensk Byggnorm 67 (Swedish Building Regulations). The National Board of Urban Planning, Stockholm, 1967.

[2] ISO/TC92, Commentary on ISO/R834 - Fire Resistance Tests of Elements of Building Construction. ISO/TC92/WG11 (Sweden-2)5, April 1972.

[3] MAGNUSSON, S.E. - PETTERSSON, O., Brandteknisk dimensionering av stålkonstruktioner (Fire Engineering Design of Steel Structures). Chapter 8 of a Manual, issued by Norrbottens Järnverk AB, Luleå, 1972.

[4] MAGNUSSON, S.E.,- PETTERSSON, O. - THOR, J., Brandteknisk dimensionering av stålkonstruktioner (Fire Engineering Design of Steel Structures). Manual, issued by the Swedish Institute of Steel Construction, Stockholm, 1974.

[5] PETTERSSON, O., Structural Fire Engineering Research Today and Tomorrow. Acta Polytechnica Scandinavica, Ci 33, Stockholm, 1965.

[6] PETTERSSON, O., Principles of Fire Engineering Design and Fire Safety of Tall Buildings. ASCE-IABSE International Con-

ference on Planning and Design of Tall Buildings, Lehigh University, Pa., August 21 - 26, 1972, Summary Report of Technical Committee 8. - Slightly modified and published as Bulletin 31, Division of Structural Mechanics and Concrete Construction, Lund Institute of Technology, Lund, 1973.

[7] PETTERSSON, O., The Connection Between a Real Fire Exposure and the Heating Conditions According to Standard Fire Resistance Tests - with Special Application to Steel Structures. CECM, Committee 3, September 1973.

[8] PETTERSSON, O., Need for and Some Remarks on Internationally Standardized Fire Test Procedures. NFPA´s First European Fire Conference, Geneva, Switzerland, October 15 - 17, 1973.

[9] THOMAS, P.H. - BALDWIN, R., Some Comments on the Choice of Failure Probabilities in Fire. Response Paper, Colloque sur les Principes de la Sécurité au Feu des Structures à Paris les 2 - 3 et 4 Juin 1971.

[10] MAGNUSSON, S.E., Probabilistic Analysis of Structural Fire Safety. ASCE National Structural Engineering Meeting, San Fransisco, California, April 9 - 13, 1973.

[11] NILSSON, L., Brandbelastning i bostadslägenheter (Fire Loads in Flats). National Swedish Institute for Building Research, Report No. 34, Stockholm, 1970.

[12] THOMAS, P.H. - HESELDEN, A.J.M. - LAW, M., Fully Developed Compartment Fires - Two Kinds of Behaviour. Fire Research Station, Borehamwood, Herts, Technical Paper No. 18, 1967.

[13] THOMAS, P.H. - HESELDEN, A.J.M., Fully-Developed Fires in Single Compartments, A Co-operative Research Programme of the Conseil International du Bâtiment (C.I.B. Report No.20). Fire Research Station, Boreham Wood, Herts, Fire Research Note No. 923, 1972.

[14] HARMATHY, T.Z., A New Look at Compartment Fires. Fire Tech-

nology, Vol. 8, No. 3, August 1972, and No. 4, November 1972.

[15] KAWAGOE, K. - SEKINE, T., Estimation of Fire Temperature-Time Curve in Rooms. Building Research Institute, Tokyo, Occasional Report No. 11, 1963. - KAWAGOE, K., Estimation of Fire Temperature-Time Curve in Rooms. Building Research Institute, Tokyo, Research Paper No. 29, 1967.

[16] ÖDEEN, K., Theoretical Study of Fire Characteristics in Enclosed Spaces. Division of Building Construction, Royal Institute of Technology, Stockholm, Bulletin No. 10, 1963.

[17] MAGNUSSON, S.E. - THELANDERSSON, S., Temperature-Time Curves for the Complete Process of Fire Development - A Theoretical Study of Wood Fuel Fires in Enclosed Spaces. Acta Polytechnica Scandinavica, Ci 65, Stockholm, 1970.

[18] MAGNUSSON, S.E. - THELANDERSSON, S., Comments on Rate of Gas Flow and Rate of Burning for Fires in Enclosures. Division of Structural Mechanics and Concrete Construction, Lund Institute of Technology, Bulleting No. 19, Lund, Sweden, 1971.

[19] NILSSON, L., Time Curve of Heat Release for Compartment Fires With Fuel of Wooden Cribs. Division of Structural Mechanics and Concrete Construction, Lund Institute of Technology, Bulletin No. 36, Lund, Sweden, 1974.

[20] THOMAS, P.H. - HINKLEY, P.L. - THEOBALD, C.R. - SIMMS, D.L., Investigations into the Flow of Hot Gases in Roof Venting. Fire Research Technical Paper No. 7, Fire Research Station, London, 1963.

[21] THOR, J., Strålningspåverkan på oisolerade eller undertaksisolerade stålkonstruktioner vid brand (Radiation Effects of Fire on Steel Structures either without Insulation or Insulated by a Ceiling). Division of Structural Mechanics and Concrete Construction, Lund Institute of Technology, Bulletin No. 29, Lund, Sweden, 1972.

[22] MAGNUSSON, S.E. - PETTERSSON, O., Kvalificerad brandteknisk dimensionering av stålbärverk (Qualified Fire Engineering Design of Load-Bearing Steel Structures). Byggmästaren No. 9, Stockholm, 1969.

[23] THOR, J., Deformations and Critical Loads of Steel Beams under Fire Exposure Conditions. National Swedish Building Research, Document D16:1973, Stockholm.

[24] DORN, J.E., Some Fundamental Experiments on High Temperature Creep. Journal of the Mechanics and Physics of Solids, Vol. 3, 1954.

[25] HARMATHY, T.Z., Deflection and Failure of Steel-Supported Floors and Beams in Fire. National Research Council, Canada, Division of Building Research, Paper No. 193, Ottawa, 1966.

[26] ROBERTSON, A.F. - RYAN, I.V., Proposed Criteria for Defining Load Failure of Beams, Floors and Roof Constructions during Fire Tests. Journal of Research, National Bureau of Standards, Vol. 63 C, Washington, 1959.

[27] DUTHEIL, J., Discussion sur le Flambement des Pièces Comprimées Axialement. L'Ossature Métallique No. 6, 1951.

[28] LARSSON, T. - PETTERSSON, O., Buckling of Fire Exposed Steel Columns, Partially Restrained with Respect to Longitudinal Expansion. Division of Structural Mechanics and Concrete Construction, Lund Institute of Technology, Bulletin No. 42, Lund, 1974.

Table 3a. Loading values to be applied in a differentiated structural fire engineering design

It is to be proved that the load-bearing structure or structural member does not collapse during the complete process of fire development for the most unfavourable combination of

(1) the dead load,

(2) the snow load, multiplied by the load factor 1.2, and

(3) the live load, multiplied by the load factor 1.4.

The dead load is determined conventionally. For the snow load, values are to be applied for the permanent and movable parts corresponding to 80 percent of the values according to the current standard specifications. For the live load, the following values are to be applied.

Type of fire compartment	Permanent loading part $kp \cdot m^{-2}$	$\{kN \cdot m^{-2}\}$	Movable loading part $kp \cdot m^{-2}$	$\{kN \cdot m^{-2}\}$
(a) Complete evacuation of occupants not certainly anticipated				
Dwellings, hotels, and hospitals	35	{0.35}	70	{0.70}
Offices, and schools	35	{0.35}	100	{1.00}
Stores, and assembly-rooms (excluding rooms with compact disposed loading)	35	{0.35}	250	{2.50}
(b) Complete evacuation of occupants certainly anticipated				
Dwellings, hotels and hospitals	35	{0.35}	35	{0.35}
Offices, and schools	35	{0.35}	55	{0.55}
Stores, and assembly-rooms (excluding rooms with compact disposed loading)	35	{0.35}	70	{0.70}

Table 4.1a. Fire load characteristics according to recent Swedish investigations - fire load density q defined according to Eq (4.1b)

Type of fire compartment	Average Mcal·m^{-2}	{MJ·m^{-2}}	Standard deviation Mcal·m^{-2}	{MJ·m^{-2}}	Design value Mcal·m^{-2}	{MJ·m^{-2}}
1 Dwellings[1)]						
1a Two rooms and a kitchen	35.8	{150}	5.9	{24.7}	40.0	{168}
1b Three rooms and a kitchen	33.1	{139}	4.8	{20.1}	35.5	{149}
2 Offices[2)]						
2a Technical offices	29.7	{124}	7.5	{31.4}	34.5	{145}
2b Administrative offices	24.3	{102}	7.7	{32.2}	31.5	{132}
2c All offices, investigated	27.3	{114}	9.4	{39.4}	33.0	{138}
3 Schools[2)]						
3a Schools - junior level	20.1	{84.2}	3.4	{14.2}	23.5	{98.4}
3b Schools - middle level	23.1	{96.7}	4.9	{20.5}	28.0	{117}
3c Schools - senior level	14.6	{61.1}	4.4	{18.4}	17.0	{71.2}
3d All schools, investigated	19.2	{80.4}	5.6	{23.4}	23.0	{96.3}
4 Hospitals	27.6	{116}	8.6	{36.0}	35.0	{147}
5 Hotels[2)]	16.0	{67.0}	4.6	{19.3}	19.5	{81.6}

1) Floor covering excluded

2) Only moveable fire load components included

Table 4.2a. Coefficient K_f for transforming a real fire load density q and a real opening factor $A\sqrt{h}/A_t$ of a fire compartment to a fictitious fire load density q_f, and a fictitious opening factor $(A\sqrt{h}/A_t)_f$, corresponding to a fire compartment, type A

$q_f = K_f\, q$ $\qquad\qquad (A\sqrt{h}/A_t)_f = K_f\, A\sqrt{h}/A_t$

Type of fire compartment	Opening factor $A\sqrt{h}/A_t$ $m^{1/2}$					
	0.02	0.04	0.06	0.08	0.10	0.12
Type A	1	1	1	1	1	1
Type B	0.85	0.85	0.85	0.85	0.85	0.85
Type C	3.0	3.0	3.0	3.0	3.0	2.5
Type D	1.35	1.35	1.35	1.50	1.55	1.65
Type E	1.65	1.50	1.35	1.50	1.75	2.00
Type F[1)]	1.00-0.50	1.00-0.50	0.80-0.50	0.70-0.50	0.70-0.50	0.70-0.50
Type G	1.50	1.45	1.35	1.25	1.15	1.05

1) The lowest value of K_f applies to a fire load density $q \geq 120$ $Mcal \cdot m^{-2}$, the highest value to a fire load density $q \leq 15$ $Mcal \cdot m^{-2}$. For intermediate fire load densities, linear interpolation gives sufficient accuracy.

The different types of fire compartment are defined as follows

Fire compartment, type B: Bounding structures of concrete.

Fire compartment, type C: Bounding structures of lightweight concrete (density $\rho = 500$ $kg \cdot m^{-3}$).

Fire compartment, type D: 50 % of the bounding structures of concrete, and 50 % of lightweight concrete (density $\rho = 500$ $kg \cdot m^{-3}$).

Fire compartment, type E: Bounding structures with the following percentage of bounding surface area:
50 % lightweight concrete (density $\rho = 500$ $kg \cdot m^{-3}$),
33 % concrete,
17 % of from the interior to the exterior: plasterboard panel (density $\rho = 790$ $kg \cdot m^{-3}$), 13 mm in thickness - diabase wool (density $\rho = 50$ $kg \cdot m^{-3}$), 10 cm in thickness - brickwork (density $\rho = 1800$ $kg \cdot m^{-3}$), 20 cm in thickness.

Table 4.2a cont.

Fire compartment, type F: 80 % of the bounding structures of sheet steel, and 20 % of concrete. The compartment corresponds to a storage space with a sheet steel roof, sheet steel walls, and a concrete floor.

Fire compartment, type G: Bounding structures with the following percentage of bounding surface area:
20 % concrete,
80 % of from the interior to the exterior: double plasterboard panel (density $\rho = 790\ kg \cdot m^{-3}$), 2 x 13 mm in thickness - air space, 10 cm in thickness - double plasterboard panel (density $\rho = 790\ kg \cdot m^{-3}$), 2 x 13 mm in thickness.

For fire compartments, not directly represented in the table, the coefficient K_f can either be determined by a linear interpolation between applicable types of fire compartment in the table or be chosen in such a way as to give results on the safe side. For fire compartments with surrounding structures of both concrete and lightweight concrete, then different values can be obtained of the coefficient K_f, depending on the choice between the fire compartment types B, C, and D at the interpolation. This is due to the fact that the relationships, determining K_f, are non-linear. However, the K_f-values of the table are such that a linear interpolation always gives results on the safe side, irrespective of the alternative of interpolation chosen. In order to avoid an unnecessarily large overestimation of K_f, that alternative of interpolation is recommended which gives the lowest value of K_f.

q	$A\sqrt{h}/A_t$	F_s/V_s	ϑ_{max} ε_r 0,3	ε_r 0,5	ε_r 0,7
10 {42}	0,01	50	325	345	370
		75	365	385	405
		100	395	410	425
		125	410	425	435
		150	425	435	440
		200	435	445	445
		400	450	450	450
	0,02	50	335	380	410
		75	410	445	475
		100	445	490	520
		125	480	520	545
		150	500	540	555
		200	540	560	575
		400	575	585	585
	0,04	50	285	320	365
		75	350	400	450
		100	405	460	510
		125	450	515	555
		150	495	555	595
		200	550	605	645
		300	625	660	690
	0,06	50	235	275	330
		75	305	370	425
		100	365	410	485
		125	415	450	545
		150	450	485	580
		200	520	550	660
		300	615	680	735
	0,08	50	200	250	300
		75	270	330	400
		100	330	400	460
		125	360	450	510
		150	410	510	580
		200	480	590	660
		300	600	700	760
	0,12	50	170	200	260
		75	220	260	350
		100	240	310	400
		125	260	380	540
		150	310	430	620
		200	380	500	700
		300	450	620	800
12,5 {52,5}	0,01	50	365	385	405
		75	410	425	435
		100	430	445	450
		125	440	450	460
		150	450	455	460
		200	455	460	465
		400	465	470	470
	0,02	50	380	435	470
		75	455	500	535
		100	500	540	560
		125	525	555	575
		150	550	570	580
		200	570	590	600
		400	600	605	605
	0,04	50	340	400	450
		75	415	485	540
		100	485	550	600
		125	535	600	640
		150	570	625	665
		200	630	665	700
	0,06	50	290	335	400
		75	365	425	495
		100	425	480	560
		125	480	525	610
		150	520	560	650
		200	580	625	705
		300	670	740	770
	0,08	50	250	315	360
		75	325	400	455
		100	385	475	535
		125	435	530	600
		150	485	585	650
		200	550	660	730
		300	655	770	-
	0,12	50	200	250	330
		75	240	320	410
		100	280	400	510
		125	340	450	620
		150	380	510	690
		200	500	600	760
		300	600	720	-
15 {63}	0,01	50	400	420	440
		75	435	445	460
		100	450	460	470
		125	460	470	475
		150	470	475	480
		200	475	480	480
		400	480	485	485
	0,02	50	425	480	515
		75	500	540	565
		100	540	575	595
		125	565	600	610
		150	585	605	615
		200	605	620	625
		400	625	630	630
	0,04	50	400	455	510
		75	490	550	600
		100	550	610	655
		125	600	655	690
		150	635	680	710
	0,06	50	340	400	475
		75	425	490	575
		100	500	550	630
		125	550	600	680
		150	590	630	720
		200	650	700	755
	0,08	50	300	375	430
		75	380	465	535
		100	450	545	605
		125	500	595	670
		150	555	650	710
		200	625	725	785
	0,12	50	260	290	400
		75	340	380	500
		100	390	460	600
		125	450	540	675
		150	500	600	750
		200	575	680	-
17,5 {73,5}	0,01	25	355	385	410
		50	430	450	465
		75	460	475	480
		100	475	480	485
		125	480	485	490
		150	485	490	495
		200	485	495	500
		400	490	500	500
	0,02	50	460	515	550
		75	530	570	595
		100	565	600	615
		125	595	610	630
		150	610	620	635
		200	625	635	645
		400	635	645	645
	0,04	50	450	515	575
		75	545	600	655
		100	600	660	705
		125	650	700	740
	0,06	25	255	300	370
		50	390	455	550
		75	490	555	655
		100	565	620	710
		125	620	670	750
	0,08	50	345	435	490
		75	440	530	600
		100	500	605	670
		125	565	650	740
		150	615	705	765
	0,12	25	160	200	275
		50	275	330	450
		75	350	430	550
		100	425	505	650
		125	475	575	725
		150	525	645	775
		200	600	725	-
20 {84}	0,01	25	390	425	445
		50	465	480	490
		75	485	500	500
		100	495	505	505
		125	500	505	510
		150	505	510	510
		200	505	510	515
		400	510	515	515
	0,02	50	500	550	575
		75	560	600	620
		100	595	620	630
		125	615	630	640
		150	625	640	645
		200	635	645	650
		400	650	650	650
	0,04	50	495	565	625
		75	585	650	700
		100	650	700	740
	0,06	25	285	340	415
		50	440	505	600
		75	540	610	700
		100	615	675	755
	0,08	50	390	490	550
		75	485	590	670
		100	565	670	735
		125	630	715	790
	0,12	25	200	235	305
		50	310	375	500
		75	425	480	610
		100	490	560	700
		125	550	620	775
		150	600	685	-
22,5 {94,5}	0,01	25	430	460	480
		50	490	505	515
		75	510	515	520
		100	520	520	520
		125	520	525	525
		150	525	525	525
		200	530	530	530
		400	530	530	530
	0,02	50	530	575	605
		75	590	620	635
		100	615	635	650
		125	630	645	650
		150	645	650	655
		200	650	660	665
	0,04	50	525	600	660
		75	620	690	735
		100	680	740	760
	0,06	25	320	380	460
		50	480	550	645
		75	585	650	740
		100	655	725	785
	0,08	50	430	540	605
		75	540	650	725
		100	610	730	780
	0,12	25	215	255	350
		50	360	415	540
		75	465	540	650
		100	540	615	750
		125	625	675	800
		150	650	740	-
25 {105}	0,01	25	455	490	500
		50	510	525	530
		75	525	530	535
		100	530	535	535
		125	530	535	540
		150	535	540	540
		300	535	540	540
		400	540	540	540
	0,02	50	555	600	625
		75	610	640	650
		100	640	650	655
		125	650	655	660
	0,04	50	570	645	700
		75	650	720	760
	0,06	25	355	420	510
		50	525	600	700
		75	640	690	780
	0,08	50	480	590	655
		75	590	700	770
		100	660	775	-
	0,12	25	240	280	385
		50	400	460	590
		75	500	580	700
		100	590	655	800
		125	650	720	-
30 {126}	0,01	25	505	525	540
		50	545	555	560
		75	555	560	560
		100	560	560	560
		125	560	565	565
		150	560	565	565
		300	565	565	570
		400	565	570	570
	0,02	50	600	640	660
		75	650	670	670
		100	660	675	675
	0,04	50	630	705	750
		75	710	780	800
	0,06	25	410	500	580
		50	595	680	760
		75	705	775	-
	0,08	50	565	665	745
		75	660	775	-
	0,12	25	290	-	440
		50	460	540	650
		75	590	660	770
		100	665	740	-
45 {190}	0,12	25	425	560	640
		50	640	760	-
	0,30	25	210	270	325
		50	360	440	520
		75	450	555	640
		100	535	650	730
		125	595	735	790
90 {380}	0,30	25	425	545	635
		50	650	790	890
		75	790	-	-

Table 5a. Maximum steel temperature ϑ_{max} for a fire exposed, uninsulated steel structure at varying fire load density q ($Mcal \cdot m^{-2}$), opening factor $A\sqrt{h}/A_t$ ($m^{1/2}$), quotient F_s/V_s (m^{-1}), and resultant emissivity ε_r. Fire compartment, type A

q	$\frac{A\sqrt{h}}{A_t}$	$\frac{A_i}{V_s}$	ϑ_{max} d_i/λ_i 0,05	d_i/λ_i 0,10	d_i/λ_i 0,20	d_i/λ_i 0,30
15 {63}	0,01	100	380	325	255	215
		125	405	350	280	240
		150	420	365	300	260
		200	440	395	335	290
		300	460	430	375	335
		400	470	445	405	370
	0,02	100	390	300	220	180
		125	420	340	250	205
		150	450	360	275	225
		200	500	400	310	260
		300	550	460	370	320
		400	575	505	415	355
	0,04	125	375	270	195	155
		150	400	300	210	175
		200	450	350	250	205
		300	550	420	310	255
		400	600	475	365	300
	0,06	150	350	250	175	140
		200	400	295	210	170
		300	480	370	260	210
		400	540	420	305	245
	0,08	200	350	255	185	145
		300	425	335	225	180
		400	500	390	270	200
	0,12	300	330	250	175	140
		400	350	300	200	165
20 {84}	0,01	75	420	355	280	235
		100	440	385	315	270
		125	460	415	340	290
		150	475	430	365	320
		200	490	455	395	355
		300	500	480	440	400
		400	505	490	460	430
	0,02	75	400	315	240	190
		100	450	355	270	220
		125	480	390	300	250
		150	510	415	325	275
		200	550	470	370	310
		300	595	530	435	370
		400	615	560	475	410
	0,04	100	400	300	210	160
		125	450	340	240	190
		150	480	365	260	210
		200	540	420	310	250
		300	620	500	380	310
		400	670	555	440	360
	0,06	100	350	250	175	135
		125	390	280	200	155
		150	430	320	220	175
		200	490	370	260	210
		300	580	450	325	260
		400	640	505	380	310
	0,08	125	340	240	165	125
		150	370	260	185	150
		200	440	310	225	175
		300	530	400	280	215
		400	600	450	340	260
	0,12	200	360	250	180	140
		300	420	305	215	175
		400	460	365	250	200
25 {105}	0,01	50	430	360	275	230
		75	470	410	330	275
		100	495	445	370	320
		125	505	465	395	350
		150	515	480	420	375
		200	525	500	450	410
		400	535	530	505	480
	0,02	50	395	300	225	180
		75	455	360	280	230
		100	500	405	310	260
		125	540	445	350	300
		150	560	470	375	320
		200	595	515	420	360
		300	635	570	490	435
		400	650	605	525	470
	0,04	75	400	295	200	160
		100	450	350	240	195
		125	510	380	270	220
		150	550	420	300	250
		200	600	480	350	290
		300	680	555	425	365
		400	725	615	485	420
	0,06	75	350	245	170	130
		100	410	295	200	160
		125	455	330	230	185
		150	500	370	255	205
		200	565	430	310	245
		300	655	520	380	305
		400	710	580	440	360
	0,08	100	350	255	175	140
		125	400	290	195	155
		150	450	325	220	175
		200	500	380	260	210
		300	600	470	340	265
		400	675	540	390	315
	0,12	150	360	245	175	140
		200	430	300	210	165
		300	510	370	260	210
		400	570	430	300	240
30 {126}	0,01	25	390	310	225	180
		50	480	410	320	270
		75	515	460	380	315
		100	535	490	420	365
		125	540	510	450	400
		150	550	525	470	425
		200	555	535	500	460
		400	560	555	540	520
	0,02	25	325	240	165	130
		50	440	345	250	200
		75	510	405	305	250
		100	550	450	350	290
		125	580	490	385	325
		150	605	520	420	355
		200	630	560	470	400
		300	665	610	540	470
		400	675	640	570	515
	0,04	50	370	270	185	140
		75	450	340	240	185
		100	510	400	280	220
		125	560	440	310	250
		150	600	475	350	285
		200	660	540	400	330
		300	730	615	485	405
		400	760	670	540	460
	0,06	75	395	280	190	150
		100	460	335	230	180
		125	510	375	265	210
		150	550	415	290	235
		200	620	475	345	275
		300	710	570	425	350
		400	765	635	490	405
	0,08	75	350	245	170	130
		100	410	295	200	160
		125	455	330	230	180
		150	500	370	255	205
		200	570	425	300	245
		300	670	525	390	305
		400	740	600	450	365
	0,12	100	340	240	155	125
		125	375	260	175	140
		150	420	290	200	160
		200	500	350	240	190
		300	600	440	300	250
		400	675	500	350	280
35 {147}	0,02	25	360	260	185	145
		50	490	380	270	225
		75	550	445	340	280
		100	595	490	385	325
		125	625	535	425	360
		150	645	555	460	395
		200	665	600	510	445
		300	690	640	580	515
		400	700	670	610	560
	0,04	25	275	200	130	100
		50	410	300	205	160
		75	500	380	265	210
		100	560	440	310	250
		125	610	480	350	280
		150	650	525	385	310
		200	700	590	445	370
		300	760	665	530	450
		400	-	710	585	510
	0,06	50	350	250	165	125
		75	430	320	215	170
		100	500	370	255	200
		125	555	415	295	235
		150	595	455	320	260
		200	660	520	380	305
		300	750	610	465	380
		400	800	675	530	440
	0,08	75	380	275	185	145
		100	450	325	220	175
		125	500	365	255	200
		150	540	405	280	225
		200	610	470	340	265
		300	715	570	430	345
		400	-	640	490	400
	0,12	100	375	265	170	135
		125	420	290	195	155
		150	465	325	225	180
		200	545	390	265	210
		300	645	480	335	275
		400	705	545	390	315
40 {168}	0,02	25	400	300	210	165
		50	530	425	310	250
		75	595	495	380	315
		100	635	545	435	360
		125	665	580	480	400
		150	680	610	510	435
		200	700	645	560	490
		300	720	680	625	550
		400	725	700	650	600
	0,04	25	300	220	145	115
		50	445	330	225	180
		75	525	400	290	235
		100	595	465	340	270
		125	645	510	380	310
		150	680	550	420	340
		200	730	615	475	395
		300	790	695	565	480
		400	-	740	630	545
	0,06	50	385	275	185	140
		75	475	350	235	185
		100	540	405	280	225
		125	595	450	325	255
		150	640	490	355	285
		200	705	560	415	335
		300	790	660	500	415
		400	-	720	565	480
	0,08	50	340	240	155	120
		75	425	300	205	160
		100	500	355	250	195
		125	550	400	280	220
		150	600	450	310	250
		200	675	505	370	300
		300	760	600	470	380
		400	-	690	530	445
	0,12	75	340	240	160	120
		100	410	290	185	145
		125	465	320	215	170
		150	510	360	250	200
		200	590	430	290	235
		300	690	520	370	300
		400	735	590	430	350
45 {190}	0,02	25	445	330	230	180
		50	570	460	340	275
		75	640	540	415	340
		100	670	580	470	395
		125	695	620	510	440
		150	710	650	550	475
		200	725	680	600	530
		300	740	710	655	600
		400	745	730	680	640
	0,04	25	330	245	160	125
		50	480	360	250	195
		75	565	440	315	250
		100	630	500	370	300
		125	680	550	410	340
		150	715	590	450	370
		200	765	650	510	430
		300	-	725	600	510
		400	-	770	655	580
	0,06	25	280	195	125	95
		50	420	300	200	155
		75	510	380	260	205
		100	585	440	310	245
		125	640	490	350	280
		150	685	530	390	310
		200	750	600	450	370
		300	-	700	540	455
		400	-	765	610	520
	0,08	50	375	260	175	135
		75	465	335	225	180
		100	530	395	270	210
		125	590	445	305	240
		150	640	490	340	275
		200	710	550	395	315
		300	800	650	500	400
		400	-	725	555	475
	0,12	75	370	260	170	130
		100	445	315	200	155
		125	510	350	235	185
		150	555	395	275	220
		200	635	470	320	260
		300	735	560	405	325
		400	790	635	470	385
	0,30	150	325	215	140	115
		200	385	265	170	135
		300	475	340	225	175
		400	545	400	270	210

Table 6a.

...../2

q	$\frac{A\sqrt{h}}{A_t}$	$\frac{A_i}{V_s}$	ϑ_{max} d_i/λ_i 0,05	d_i/λ_i 0,10	d_i/λ_i 0,20	d_i/λ_i 0,30
50 {210}	0,02	25	480	355	250	200
		50	605	490	375	300
		75	665	570	450	380
		100	700	620	510	435
		125	720	650	550	475
		150	730	675	585	510
		200	745	700	630	565
		300	755	735	680	635
	0,04	25	350	255	170	135
		50	500	385	270	210
		75	600	460	340	265
		100	655	525	395	315
		125	705	575	435	355
		150	740	615	475	395
		200	785	675	540	450
		300	-	750	625	545
		400	-	795	690	600
	0,06	25	300	210	135	105
		50	445	320	215	170
		75	540	400	275	220
		100	610	465	330	260
		125	665	515	375	300
		150	710	560	410	330
		200	775	625	475	395
		300	-	725	570	480
		400	-	790	635	545
	0,08	25	260	180	115	90
		50	400	275	180	140
		75	500	350	240	190
		100	555	410	290	225
		125	615	460	325	255
		150	665	505	355	295
		200	750	580	425	350
		300	-	680	525	430
		400	-	750	595	500
	0,12	50	320	220	145	110
		75	410	290	185	145
		100	480	345	225	175
		125	550	390	260	200
		150	600	430	295	235
		200	675	500	350	280
		300	780	600	440	350
		400	-	680	510	415
	0,30	125	305	205	135	110
		150	350	230	150	125
		200	410	285	185	145
		300	500	365	245	190
		400	575	425	290	225
60 {250}	0,02	25	550	420	295	235
		50	665	560	430	350
		75	715	640	515	435
		100	745	675	570	495
		125	760	705	610	540
		150	770	725	640	575
		200	780	750	690	625
	0,04	25	405	300	200	150
		50	560	430	305	240
		75	650	515	380	310
		100	715	580	440	360
		125	755	640	490	405
		150	790	675	530	440
		200	-	730	600	505
		300	-	795	680	590
	0,06	25	345	240	155	120
		50	500	360	240	195
		75	600	450	315	250
		100	670	515	375	300
		125	725	570	415	340
		150	765	615	460	375
		200	-	685	525	435
		300	-	775	625	530
		400	-	-	695	600
	0,08	25	300	200	135	100
		50	450	315	210	160
		75	550	400	275	210
		100	615	460	325	255
		125	680	515	365	290
		150	725	560	400	330
		200	800	640	475	390
		300	-	750	580	480
		400	-	-	650	550
	0,12	50	370	250	160	125
		75	470	330	210	170
		100	550	385	250	200
		125	600	430	300	235
		150	650	480	330	265
		200	735	550	400	310
		300	-	660	500	400
		400	-	750	575	465
	0,30	125	345	235	155	125
		150	395	265	175	145
		200	460	325	215	165
		300	555	410	280	220
		400	630	475	330	260
75 {315}	0,04	25	525	395	270	205
		50	665	540	400	320
		75	735	625	490	400
		100	790	680	550	455
		125	-	710	600	505
		150	-	750	640	550
		200	-	800	695	605
	0,06	25	400	280	185	140
		50	565	415	285	225
		75	670	510	365	290
		100	740	585	425	345
		125	790	640	480	390
		150	-	685	525	430
		200	-	755	595	500
		300	-	-	695	600
	0,08	25	350	240	160	120
		50	510	365	250	190
		75	615	455	320	250
		100	700	530	375	300
		125	750	585	425	340
		150	800	640	470	385
		200	-	710	545	450
		300	-	-	650	550
		400	-	-	730	625
	0,12	50	420	290	190	150
		75	525	375	250	200
		100	600	440	300	240
		125	680	500	350	275
		150	725	550	390	300
		200	800	620	450	360
		300	-	730	550	450
		400	-	800	650	530
	0,30	75	305	205	135	105
		100	365	250	165	130
		125	410	285	190	150
		150	465	315	210	170
		200	535	385	255	200
		300	635	480	335	260
		400	715	550	390	310
90 {380}	0,04	25	630	480	330	260
		50	760	640	490	395
		75	-	725	590	490
		100	-	770	650	560
		125	-	790	700	610
		150	-	-	730	650
	0,06	25	450	315	210	160
		50	625	470	325	255
		75	730	570	410	330
		100	795	640	475	390
		125	-	700	530	435
		150	-	745	575	480
		200	-	-	650	550
		300	-	-	750	665
	0,08	25	400	275	180	140
		50	570	415	285	220
		75	680	510	360	285
		100	755	590	420	340
		125	-	650	480	390
		150	-	700	520	430
		200	-	775	600	500
		300	-	-	700	600
	0,12	25	320	220	140	105
		50	475	330	220	175
		75	590	425	285	225
		100	670	495	340	275
		125	740	550	395	305
		150	800	600	440	350
		200	-	680	500	405
		300	-	800	605	505
		400	-	-	700	595
	0,30	75	355	245	160	125
		100	425	290	195	150
		125	480	335	225	175
		150	530	375	250	195
		200	610	445	300	235
		300	720	545	385	305
		400	800	625	455	360
120 {500}	0,04	25	660	500	350	270
		50	-	670	520	420
		75	-	760	620	520
		100	-	-	695	595
		125	-	-	745	650
	0,06	25	550	395	265	200
		50	735	570	400	320
		75	-	675	500	405
		100	-	750	575	475
		125	-	800	635	535
		150	-	-	685	580
		200	-	-	755	655
	0,08	25	475	325	220	165
		50	660	490	340	260
		75	770	595	435	340
		100	-	670	505	400
		125	-	740	560	450
		150	-	780	610	500
		200	-	-	690	580
	0,12	25	390	250	165	130
		50	565	390	260	210
		75	690	495	340	270
		100	760	565	400	320
		125	-	640	450	370
		150	-	690	500	410
		200	-	760	575	480
		300	-	-	700	590
	0,30	75	435	300	195	150
		100	510	355	235	180
		125	575	410	270	210
		150	625	455	305	240
		200	705	530	365	285
		300	-	640	465	370
		400	-	720	540	435

Table 6a. Maximum steel temperature ϑ_{max} for a fire exposed, insulated steel structure at varying fire load density q (Mcal·m^{-2}), opening factor $A\sqrt{h}/A_t$ (m$^{1/2}$), quotient A_i/V_s (m^{-1}), and quotient d_i/λ_i (m^2·°C·h·kcal^{-1}). Fire compartment type A

q	$\frac{A\sqrt{h}}{A_t}$	$\frac{A_i}{V_s}$	ϑ_{max} d_i 30	d_i 50	d_i 70
20 {84}	0,01	200	325	250	200
		300	380	300	245
		400	415	335	275
	0,02	200	295	215	165
		300	355	265	210
		400	400	300	240
	0,04	300	300	205	150
		400	350	250	180
	0,06	400	320	200	135
25 {105}	0,01	125	330	250	200
		150	355	270	225
		200	395	315	260
		300	450	370	310
		400	480	405	340
	0,02	150	300	225	175
		200	350	260	205
		300	415	315	250
		400	465	355	285
	0,04	200	300	210	150
		300	375	265	195
		400	430	310	225
	0,06	300	330	210	150
		400	390	250	170
30 {126}	0,01	75	310	230	175
		100	355	270	215
		125	390	305	245
		150	420	335	270
		200	460	375	315
		300	500	425	365
		400	520	460	405
	0,02	125	320	235	185
		150	355	260	205
		200	405	305	240
		300	480	370	300
		400	530	420	335
	0,04	150	300	210	155
		200	350	250	185
		300	440	315	235
		400	500	365	270
	0,06	200	305	200	140
		300	395	250	180
		400	450	300	210
	0,08	300	330	210	150
		400	390	250	175
35 {147}	0,02	100	325	240	190
		125	365	270	215
		150	405	300	240
		200	455	350	280
		300	535	420	340
		400	575	470	385
	0,04	125	300	215	155
		150	340	240	180
		200	400	290	215
		300	490	355	270
		400	550	410	310
	0,06	150	300	190	145
		200	350	235	165
		300	450	300	210
		400	500	350	250
	0,08	200	300	200	135
		300	385	250	175
		400	450	300	200
40 {168}	0,02	100	370	275	215
		125	415	310	245
		150	455	345	270
		200	515	400	320
		300	585	475	390
		400	625	525	435
	0,04	100	300	205	155
		125	340	240	180
		150	380	270	205
		200	450	320	240
		300	535	400	300
		400	600	450	350
	0,06	125	295	195	140
		150	330	220	165
		200	400	265	200
		300	495	340	240
		400	550	395	285
	0,08	200	350	225	155
		300	440	280	200
		400	500	340	230
45 {190}	0,02	75	365	265	205
		100	430	315	250
		125	480	360	290
		150	520	400	320
		200	580	460	370
		300	645	540	450
		400	680	590	500
	0,04	100	325	230	175
		125	375	265	200
		150	415	300	225
		200	485	350	270
		300	580	435	335
		400	640	495	385
	0,06	125	325	220	160
		150	365	250	185
		200	435	300	220
		300	535	375	275
		400	600	430	320
	0,08	150	320	210	150
		200	385	250	175
		300	480	315	225
		400	550	375	260
	0,12	300	325	230	175
		400	375	270	200
50 {210}	0,02	50	320	225	175
		75	410	300	235
		100	475	355	280
		125	530	400	320
		150	565	445	360
		200	620	500	415
		300	680	580	490
		400	710	625	545
	0,04	75	300	210	160
		100	355	255	190
		125	410	300	225
		150	455	330	250
		200	525	390	300
		300	620	475	365
		400	680	535	420
	0,06	100	310	210	155
		125	360	240	175
		150	400	275	205
		200	475	325	240
		300	575	410	300
		400	640	475	350
	0,08	125	310	210	150
		150	355	235	170
		200	425	285	200
		300	530	355	260
		400	600	420	300
	0,12	200	295	200	150
		300	365	255	200
		400	425	300	230
60 {250}	0,02	50	400	285	220
		75	500	375	295
		100	565	440	350
		125	610	495	400
		150	640	530	440
		200	690	595	505
		300	735	660	580
		400	760	695	625
	0,04	75	355	250	190
		100	425	305	230
		125	485	350	270
		150	525	390	300
		200	600	450	350
		300	690	550	430
		400	740	600	485
	0,06	75	300	200	150
		100	360	250	185
		125	415	285	215
		150	465	325	240
		200	540	385	285
		300	650	475	360
		400	710	540	415
	0,08	100	320	215	150
		125	370	250	180
		150	415	285	200
		200	500	340	250
		300	605	435	305
		400	680	500	350
	0,12	200	350	230	175
		300	445	295	225
		400	505	350	265
75 {315}	0,04	50	340	240	180
		75	450	315	245
		100	525	385	295
		125	580	435	340
		150	620	490	375
		200	695	555	440
		300	780	650	525
		400	-	700	580
	0,06	75	360	250	185
		100	440	300	225
		125	500	350	260
		150	550	390	295
		200	630	460	350
		300	730	560	435
		400	795	630	495
	0,08	75	320	215	155
		100	395	265	190
		125	450	305	225
		150	500	350	250
		200	580	410	300
		300	700	520	380
		400	770	580	440
	0,12	125	305	220	160
		150	340	250	190
		200	430	300	220
		300	535	395	280
		400	610	450	325
	0,30	400	290	210	150
90 {380}	0,04	50	415	295	220
		75	540	390	300
		100	620	465	365
		125	680	530	420
		150	725	580	465
		200	785	650	540
		300	-	745	635
		400	-	800	690
	0,06	50	320	220	165
		75	425	295	220
		100	510	360	270
		125	570	410	315
		150	625	460	355
		200	710	530	420
		300	-	635	510
		400	-	700	570
	0,08	75	375	250	190
		100	450	310	230
		125	515	365	270
		150	570	400	300
		200	650	480	360
		300	765	585	450
		400	-	655	515
	0,12	100	325	230	175
		125	375	275	200
		150	425	305	230
		200	500	365	275
		300	615	475	350
		400	695	540	405
	0,30	300	290	205	160
		400	340	245	190
120 {500}	0,04	25	355	240	190
		50	560	410	315
		75	680	525	420
		100	750	610	495
		125	-	670	560
		150	-	715	610
		200	-	785	685
		300	-	-	765
		400	-	-	-
	0,06	25	260	175	130
		50	430	300	225
		75	565	400	305
		100	650	485	370
		125	725	545	425
		150	775	600	480
		200	-	675	560
		300	-	775	660
	0,08	50	360	245	185
		75	470	325	250
		100	555	400	300
		125	635	460	350
		150	690	510	395
		200	770	595	465
		300	-	705	570
		400	-	775	635
	0,12	75	350	250	190
		100	425	310	235
		125	485	360	270
		150	540	405	305
		200	620	480	365
		300	740	590	460
		400	-	660	520
	0,30	200	330	230	180
		300	420	300	235
		400	490	355	275

Table 6b. Maximum steel temperature ϑ_{max} for a fire exposed steel structure, insulated with slabs of mineral wool (type Minwool 3060 or Rockwool 337, density $\rho_i = 150$ kg·m^{-3}), at varying fire load density q (Mcal·m^{-2}), opening factor $A\sqrt{h}/A_t$ (m$^{1/2}$), quotient A_i/V_s (m^{-1}), and insulation thickness d_i (mm). Fire compartment type A

q	$\frac{A\sqrt{h}}{A_t}$	$\frac{F_s}{V_s}$	Maximum steel temperature ϑ_{max}, and ( ) maximum ceiling temperature; $(d_i/\lambda_i)_{fict}$ = 0,05	( )	0,10	( )	0,20	( )	0,30	( )
15 {63}	0,02	50	130	(470)	90	(440)	65	(410)	50	(390)
		100	180		130		90		70	
		200	230		170		115		90	
		300	260		190		130		100	
	0,04	50	100	(565)	70	(530)	45	(500)	40	(475)
		100	150		100		65		50	
		200	200		140		90		70	
		300	240		170		110		80	
	0,08	50	65	(675)	50	(630)	35	(590)	25	(570)
		100	95		70		50		40	
		200	150		100		65		50	
		300	190		125		90		60	
	0,12	50	40	(735)	35	(690)	30	(650)	25	(620)
		100	60		45		40		30	
		200	120		70		50		40	
		300	155		100		60		45	
25 {105}	0,02	50	200	(510)	140	(470)	95	(435)	75	(420)
		100	260		185		125		100	
		200	300		225		155		120	
		300	320		245		170		130	
	0,04	50	160	(600)	110	(565)	75	(530)	55	(515)
		100	230		150		100		75	
		200	290		205		135		100	
		300	325		235		155		115	
	0,08	50	115	(680)	75	(635)	50	(595)	40	(570)
		100	160		110		70		55	
		200	240		160		100		75	
		300	285		195		120		90	
	0,12	50	80	(740)	60	(690)	40	(650)	30	(620)
		100	130		80		60		45	
		200	190		125		80		60	
		300	235		160		100		75	
40 {168}	0,02	50	300	(560)	220	(520)	145	(480)	110	(460)
		100	360		260		175		135	
		200	380		290		200		160	
		300	385		295		210		165	
	0,04	50	240	(645)	160	(600)	105	(560)	80	(535)
		100	315		220		140		100	
		200	375		270		180		135	
		300	390		290		195		150	
	0,08	50	170	(715)	110	(665)	70	(625)	55	(600)
		100	245		160		100		75	
		200	335		220		140		105	
		300	380		260		165		120	
	0,12	50	130	(750)	85	(700)	55	(660)	45	(630)
		100	200		130		85		60	
		200	290		190		115		85	
		300	340		225		145		100	
60 {250}	0,02	50	435	(615)	315	(570)	200	(530)	160	(500)
		100	450		340		240		185	
		200	455		350		250		200	
		300	455		350		250		200	
	0,04	50	340	(680)	225	(630)	145	(590)	110	(560)
		100	400		285		185		140	
		200	435		320		220		165	
		300	445		330		230		180	
	0,08	50	250	(750)	160	(700)	100	(650)	75	(625)
		100	340		225		130		100	
		200	415		285		185		135	
		300	445		315		210		155	
	0,12	50	190	(780)	120	(725)	75	(680)	60	(660)
		100	285		185		110		80	
		200	375		250		155		110	
		300	420		290		185		130	
90 {380}	0,04	50	475	(740)	330	(680)	205	(630)	150	(600)
		100	510		370		250		190	
		200	515		385		270		210	
		300	515		385		270		215	
	0,08	50	345	(790)	225	(730)	130	(675)	100	(650)
		100	430		290		180		130	
		200	480		340		225		170	
		300	495		360		250		190	
120 {500}	0,04	50	560	(780)	400	(715)	260	(660)	200	(630)
		100	570		420		290		220	
		200	575		425		300		230	
		300	575		425		300		230	
	0,08	50	425	(810)	280	(750)	160	(695)	120	(670)
		100	495		345		210		160	
		200	520		375		250		195	
		300	525		385		260		205	

Table 7a. Maximum steel temperature ϑ_{max} for a steel beam construction according to Fig. 7a, fire exposed from below, at varying fire load density q (Mcal · m^{-2}), opening factor $A\sqrt{h}/A_t$ ($m^{1/2}$), quotient F_s/V_s (m^{-1}), and quotient d_i/λ_i ($m^2 \cdot {}^oC \cdot h \cdot kcal^{-1}$). The corresponding maximum temperature of the ceiling is given in a parenthesis. Slab of reinforced concrete. Fire compartment type A